1ST INTERNATIONAL CONFERENCE ON PHONONIC CRYSTALS, METAMATERIALS & OPTOMECHANICS

Extended Abstracts

Track 3: Periodic Structures

Phononics 2011: First International Conference on Phononic Crystals, Metamaterials and Optomechanics
Santa Fe, New Mexico, USA, May 29-June 2, 2011
PHONONICS-2011-0009

Elastic waves in a three-dimensional hexagonal close-packed granular crystal: observation of rotational modes and nonlinear effects

A. Merkel[1], V. Tournat[1*], V. Gusev[2]
[1]LAUM, [2]LPEC, CNRS, Université du Maine, Le Mans, France.
aurelien.merkel.etu@univ-lemans.fr, vincent.tournat@univ-lemans.fr,
vitali.goussev@univ-lemans.fr

Abstract: Noncohesive granular phononic crystals show peculiar features related to the elastic nonlinearities at the contacts and the rotational degrees of freedom of the grains. Evidence of rotational mode propagation and non reciprocity for nonlinear acoustic effects is found in a hexagonal close-packed crystal layer with a gravity-induced elasticity gradient.

Noncohesive granular crystals are periodic arrangements of elastic spheres with noncohesive contacts [1,2]. Due to the intrinsic elastic nonlinearity of the interaction between the beads, these media are found to exhibit an overall high nonlinearity[3]. Moreover, the fact that the grains are spherical and weakly frustrated for rotation due to the non cohesive character of the arrangement, provides appropriate conditions for the observation of rotational modes of propagation and coupled rotational-transverse modes[2,4,5].

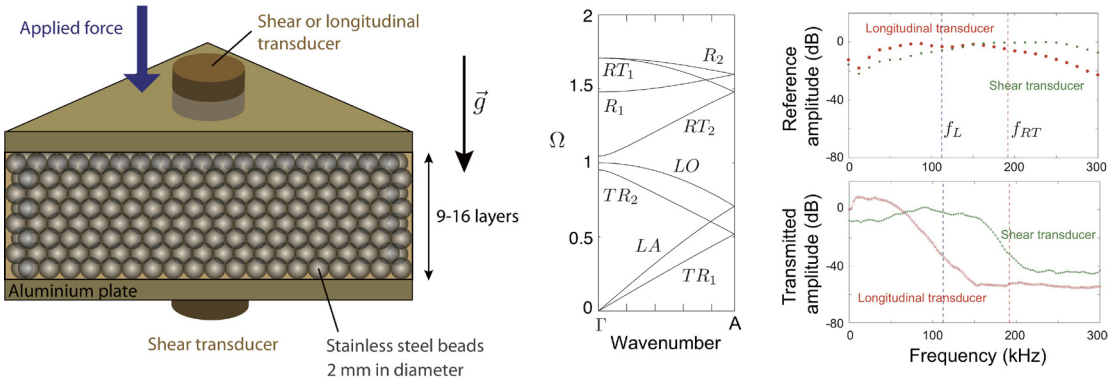

Figure 1: (left) Schematics of the experimental setup. (center) Normalized dispersion curves in the z direction. (right) Reference and transmitted amplitude through the granular layer for shear and longitudinal detection.

The theory developed in Ref. 2, taking into account friction and the rotational degrees of freedom, shows that there should exist in the z direction, longitudinal modes (LA and LO), transverse-rotational modes (TR_1 and TR_2), rotational-transverse (RT_1 and RT_2) and pure rotational modes (R_1 and R_2), see Fig. 1 (center). When shear and longitudinal waves are excited from one side of the granular crystal layer, a pass-band up to f_L (predicted here for an applied static force of 780 N) is observed for

Phononics 2011: First International Conference on Phononic Crystals, Metamaterials and Optomechanics
Santa Fe, New Mexico, USA, May 29-June 2, 2011
PHONONICS-2011-0009

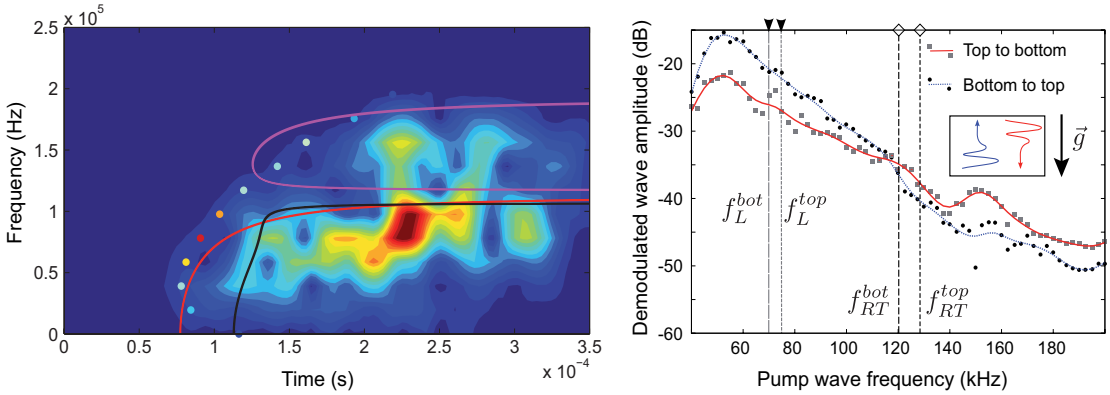

Figure 2: (left) Spectrogram of a wide-frequency-band pulse transmitted through the layer. (right) Demodulated wave amplitude for bottom-to-top and top-to-bottom paths of propagation.

longitudinal waves (detection with the longitudinal transducer, Fig. 1 (right)). With shear detection, a pass-band up to f_{RT} (cut-off frequency for rotational-transverse modes) is observed, showing that the higher frequency modes associated to rotation of the beads propagate. Complementary experimental results will be discussed, such as the static pressure dependence of the cut-off frequencies.

In Fig. 2 (left), the theoretical group delays for the detectable modes (L, TR, RT, shown as lines) are compared to the energy front arrival time of the transmitted energy and are in qualitative agreement for both longitudinal and rotational-transverse modes, confirming the role of the rotational degree of freedom. Non reciprocity for nonlinear effects is finally reported in Fig. 2 (right). Wave packets are generated by a transducer and then are nonlinearly self-demodulated in the medium[6]. This frequency-down conversion does not exhibit the same efficiency for propagative or evanescent pump waves and is direction dependent. This phenomenon is explained by the existence of a vertical gradient of medium properties, induced by gravity, both for the wave attenuation and the nonlinearity of the medium. We believe that our experiments provide the first experimental evidence of the dependence of nonlinear acoustic phenomena on propagation direction in spatially inhomogeneous granular media.

This work is supported by ANR grant STABINGRAM.

References

[1] A. Merkel, V. Tournat, V.E. Gusev, Ultrasonics 50, 133-138 (2009).
[2] A. Merkel, V. Tournat, V.E. Gusev, Phys. Rev. E 82, 031305 (2010).
[3] V. Tournat, V.E. Gusev, Acta-Acustica united with Acustica 96, 208-224 (2010).
[4] E. Cosserat, F. Cosserat, Théorie des Corps déformables (Herman et fils, Paris, 1909).
[5] A. C. Eringen, Microcontinuum Field Theories.1 : Foundations and Solids (Springer Verlag Inc., New York, 1999).
[6] V. Tournat, B. Castagnède and V.E. Gusev, Phys. Rev. E 70, 056603 (2004).

Phononics 2011: First International Conference on Phononic Crystals, Metamaterials and Optomechanics
Santa Fe, New Mexico, USA, May 29-June 2, 2011
PHONONICS-2011-0011

Out-of-plane acoustic modes in monolayer phononic granular membranes

I. Perez-Arjona[1], A. Merkel[2], V. Tournat[2*], V. Gusev[3], V. Sanchez-Morcillo[1]
[1]IGIC, Universidad Politècnica de Valencia, 46730 Grau de Gandia, Spain.
[2]LAUM, [3]LPEC, CNRS, Université du Maine, Le Mans, France.
[*]vincent.tournat@univ-lemans.fr

Abstract: Waves in hexagonal monolayer granular membranes are studied theoretically. The predicted propagation modes involve an out-of-plane displacement and two rotations with axes in the membrane plane. Shear and bending rigidities at the contact are considered, as well as coupling with a substrate. Dispersion relations and band gaps are presented and discussed for various contact properties.

Recently, ordered monolayer nanoparticle arrays have been successfully produced by self-assemblage during a drying process[1], and can be stretched across micrometer size holes to provide freely suspended monolayer membranes[2,3]. Such granular membranes, with peculiar elastic and optical properties could lead to a wide range of sensor applications. Here, we report a theoretical work on the vibrational properties of such granular membranes. The specificities of these granular systems compared to classical membranes come from the particle finite dimensions and their finite rotational inertia (rotational degree of freedom) which lead to elastic interactions through non-central forces. In particular, it provides in addition to shear and longitudinal acoustic modes, the existence of rotational (or so-called micro-rotational) modes[4–6].

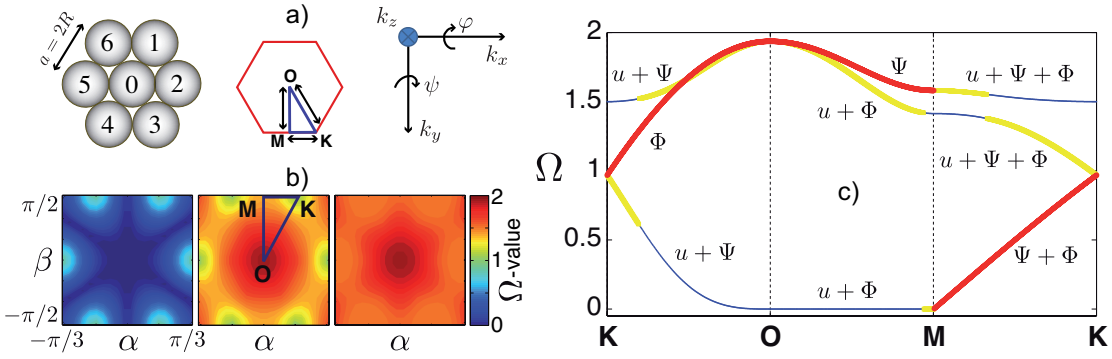

Figure 1: a) Geometrical arrangement of the beads in the elementary cell of the hexagonal membrane crystal and definition of the Brillouin zone and coordinate axes. b) Iso-surface plots of the lowest eigenvalue $\Omega = \omega^2/(4\xi/m)$ of the dynamical matrix (left), the middle eigenvalue (center) and the largest eigenvalue (right) ($\alpha = k_x/4$ and $\beta = \sqrt{3}k_y/4$). c) Dispersion relations and associated symmetries of the modes.

In order to model out-of-plane mode propagation in monolayer granular membranes, the equations of motion for the displacement u_0 of the center of the central particle 0, and

Phononics 2011: First International Conference on Phononic Crystals, Metamaterials and Optomechanics
Santa Fe, New Mexico, USA, May 29-June 2, 2011
PHONONICS-2011-0011

the equations for the rotations φ_0 and ψ_0 (defined in Fig. 1(a)) are written in the form

$$m\ddot{u}_0 = -\xi\left[(\delta u_1 + \delta u_4) + (\delta u_3 + \delta u_6) + (\delta u_2 + \delta u_5)\right], \quad (1)$$

$$I\ddot{\varphi}_0 = \frac{\sqrt{3}}{2}\xi R\left[(\delta u_1 - \delta u_4) - (\delta u_3 - \delta u_6)\right], \quad (2)$$

$$I\ddot{\psi}_0 = \frac{R}{2}\xi\left[(\delta u_1 - \delta u_4) + (\delta u_3 - \delta u_6)\right] + R\xi\left[\delta u_2 - \delta u_5\right], \quad (3)$$

where m is the mass of the particle, ξ is the contact shear rigidity and, for the particular case of homogeneous spheres, the momentum of inertia is $I = \frac{2}{5}mR^2$. The terms δu_i denote elongations of the spring at the contact between the central and $i-$particle, that is, the relative displacement between 0 and $i-$particle at the contact point.

After plane wave substitution, the dynamic matrix is obtained whose eigenvalues provide the dispersion relations plotted in Fig. 1(c) in the case where only shear rigidity between spheres is taken into account. Pure rotational modes are predicted in both x and y propagation directions, as well as a zero frequency mode along the path OM.

Fig. 2 shows an example of the modified dispersion relations when bending rigidity at the contacts is introduced.

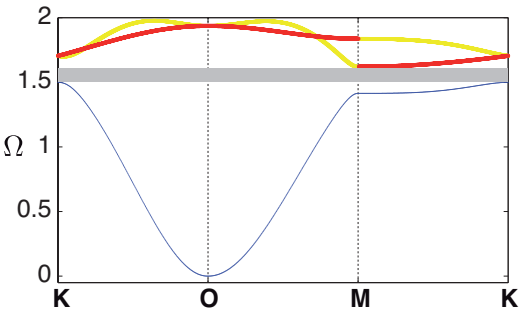

Figure 2: Dispersion relations obtained when shear and bending rigidities at the contacts are taken into account. Here a bending rigidity of 0.7 times the shear rigidity is used. An absolute band gap appears starting from a bending to shear rigidity ratio of 8/15. The zero frequency mode of Fig. 1 when bending is neglected is not predicted anymore.

Furthermore, the influence of the interaction with a rigid substrate has been taken into account. It is expected that these results will be useful for describing the phonon transport in two-dimensional nano-crystals, and vibration properties of micrometer scale granular membranes potentially used as sensors in the near future.

This work is supported by ANR grant STABINGRAM.

References

[1] T. P. Bigioni et al., Nature Materials 5, 265-270 (2006).
[2] K. E. Mueggenberg et al., Nature Materials 6, 656-660 (2007).
[3] W. Cheng et al., Nature Materials 8, 519-525 (2009).
[3] E. Cosserat, F. Cosserat, Théorie des Corps déformables (Herman et fils, Paris, 1909).
[4] A. C. Eringen, Microcontinuum Field Theories.1 : Foundations and Solids (Springer Verlag Inc., New York, 1999).
[5] A. Merkel, V. Tournat, V.E. Gusev, Ultrasonics 50, 133-138 (2009).

Phononics 2011: First International Conference on Phononic Crystals, Metamaterials and Optomechanics
Santa Fe, New Mexico, USA, May 29-June 2, 2011
PHONONICS-2011-0018

2D Wave Propagation in Periodically Layered Composite Structures with Damages

Mikhail V. Golub[1] , **Chuanzeng Zhang**[2]

[1] *Institute for Mathematics, Mechanics and Informatics, Kuban State University, Stavropolskaya Str. 149, 350040 Krasnodar, Russian Federation*
m_golub@inbox.ru
[2] *Department of Civil Engineering, University of Siegen, D-57068 Siegen, Germany*
c.zhang@uni-siegen.de

Abstract: Plane SH-wave propagation in periodically layered elastic composites with a single strip-like crack and an array of cracks (periodic or stochastic) is investigated using the transfer matrix method and the boundary integral equation method. The focus of this analysis is on the wave transmission and reflection, band gaps, localization and resonance phenomena due to crack-like damages.

Wave propagation in periodic composite structures is usually accompanied by localization phenomena and band-gaps, which are observed in photonic and phononic crystals[1]. Elastic waveguides are susceptible to damages like cracks during the manufacturing or in service. In particular, the delamination at imperfect interfaces between the constituents, interior cracks in the individual layers can occur. Such interface or interior damages could change the dynamic properties of the periodic composites and correspondingly cause noticeable alterations in band gaps and wave transmission spectra etc. To simplify the analysis, imperfect interfaces are usually simulated by a periodic/stochastic distribution of interface cracks or by spring boundary conditions[2;3], where the latter in a limiting case corresponds to a crack. Several analytical and numerical approaches have been developed so far for wave propagation analysis in periodic structures[4] including the transfer matrix method employed in the present work. Wave propagation and diffraction by a crack in multilayered composite structures can be efficiently investigated by using integral representations and Green's functions in conjunction with the integral-transform technique[5].

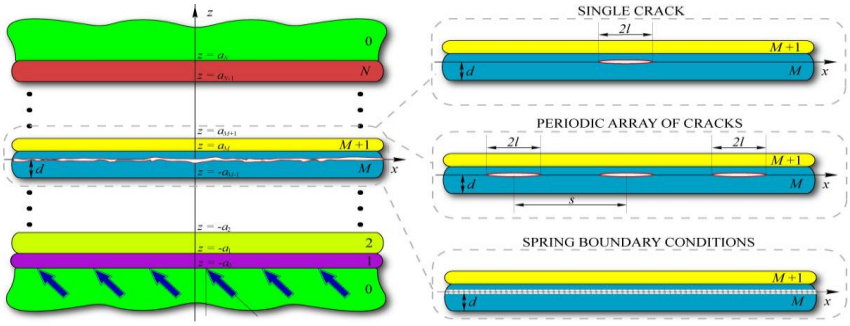

Figure 1 Geometry of the problem and mathematical model of a multi-layered composite between two identical half-planes with a damaged zone (a single crack, a periodic array of cracks, and a spring model).

In this paper, we consider time-harmonic plane wave propagation with circular frequency ω in a layered waveguide composed of two half-planes with a set of N elastic layers and one damaged layer in the stack. The Cartesian coordinate system $\boldsymbol{x}=(x,z)$ associated with the damaged zone is introduced: the Ox axis and the damaged interface are assumed to be parallel to the interfaces between the layers. The i-th layer occupying the domain $|x|<\infty$, $a_{i-1}<z<a_i$ of the thickness $d_i=a_i-a_{i-1}$ has the shear modulus μ_i and the mass density ρ_i. The damage is situated in the M-th layer at a distance d from the interface $z=a_{M-1}$. The following three damage types are considered here: a single strip-like crack of length $2l$, a periodic array of cracks of length $2l$ with a crack-distance s, and distributed damages modeled by spring boundary conditions[3] (see Figure 1). The problem for a single crack and for an array of cracks is solved by using a boundary integral equation method for the unknown crack-opening-displacement (COD), while the application of the spring boundary conditions allows us to use the T-matrix method with an approximate estimation of the spring stiffness[3].

Numerical examples will be presented to show the resonant and non-resonant regimes of the wave motion in the periodically layered composites weakened by a single strip-like crack or a periodic array of cracks and wave localization in the vicinity of the damages. Wave motion with large amplitudes for

Phononics 2011: First International Conference on Phononic Crystals, Metamaterials and Optomechanics
Santa Fe, New Mexico, USA, May 29-June 2, 2011
PHONONICS-2011-0018

some parameter combinations is found through the analysis of the COD, and it is shown that such resonant regimes are quite different within band gaps and pass bands. Dynamic stress intensity factors (SIFs), average energy density flow, energy transmission coefficient κ^+ and average COD normalized by the amplitude of the incident wave field v_u are also investigated to gain a better understanding of the wave propagation processes. If cracks are present in the layered composites, then the local maxima and minima of the COD and the SIFs are related to the maxima of the energy amount transferred through the layered composites, to be more precise, the extremal values of these quantities occur at the same frequencies in the pass bands. On the other hand, the amplitude of the wave motion at frequencies within the band gaps decreases rapidly in the direction of wave propagation, whereas the presence of cracks may cause noticeably larger amplitudes of the wave motion in their vicinity, i.e., wave localization. Stress and displacement fields of largest amplitudes are observed at resonance frequencies.

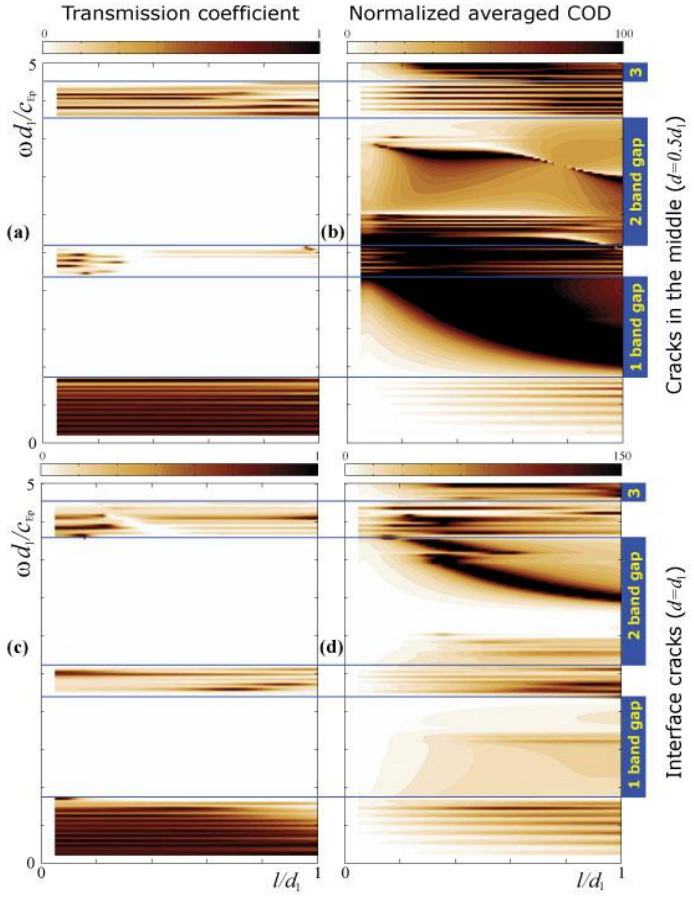

Figure 2 The transmission coefficient $\kappa^+(\omega,l)$ **(a,c)** and the normalized average COD $v_u(\omega,l)$ **(b,d)** for a periodic array of cracks with $s=3$ and situated in the middle of the 15-th layer**(a,b)** and at the interface between the 15-th and 16-th layer **(c,d)**. Band gaps are marked.

Without loss of generality we assume 32 layers in a waveguide and a unit-cell composed of 2 layers (Plumbum/Epoxy), and the damaged layer is in the middle of the stack of layers $M=15$. A single crack does not influence the band gaps due to the attenuation of the scattered wave field, while it changes, of course, wave pattern in the vicinity of the crack. Within the pass bands two kinds of resonances with intensified wave motion in the vicinity of the crack are observed.

An illustration example is given in Figure 2, where the transmission coefficient $\kappa^+(\omega,l)$ and the normalized average of COD $v_u(\omega,l)$ for a normally incident SH-wave are presented. Obviously, the presence of a damaged zone can only extend the band gaps, while for a periodic array of cracks two types of resonances are also observed. A "weak" resonance is observed in the pass bands, and it corresponds to relatively high amplitudes. A "strong" resonance is noted within the bang gaps, which is characterized by dark zones in Figs. 2**(b)** and 2**(d).** The "strong" resonances are induced by the localization of the wave motion near the damages.

The work is supported by the Ministry of Education and Science of Russian Federation, the German Research Foundation (DFG, Project No. ZH 15/11-1) and the German Academic Exchange Service DAAD, which are gratefully acknowledged.

References

[1] P. G. Martinsson, A. B. Movchan, *Quarterly Journal of Mechanics and Applied Mathematics*. **56**, 45-64 (2003).
[2] J. Baik, R. Thompson, *Journal of Nondestructive Evaluation*, **4**, 177-196 (1984).
[3] A. Boström, M.V. Golub, *Quarterly Journal of Mechanics and Applied Mathematics*, **62**, 39-52 (2009).
[4] M. Sigalas et. al., *Zeitschrift fur Kristallographie,* **220**, 765-809 (2005).
[5] E.V. Glushkov, N.V. Glushkova, *Journal of Computational Acoustics*, **9(3)**, 889-898 (2001).

Phononics 2011: First International Conference on Phononic Crystals, Metamaterials and Optomechanics
Santa Fe, New Mexico, USA, May 29-June 2, 2011
PHONONICS-2011-0030

Tailoring Stress Waves in 2-D Highly Nonlinear Granular Crystals: Simulations and Experiments

Andrea Leonard[1], Amnaya Awasthi[2], Philippe Geubelle[2], Chiara Daraio[1]

[1] Division of Engineering and Applied Sciences
California Institute of Technology, Pasadena CA, USA
andreal@caltech.edu, daraio@caltech.edu
[2] Dept. of Aerospace Engineering and Dept. of Computational Sciences and Engineering
University of Illinois Urbana Champaign, IL, USA
amnaya@illinois.edu, geubelle@illinois.edu

Abstract: We study the propagation of elastic stress waves in two-dimensional highly nonlinear granular crystals composed of square packings of spheres with and without cylindrical intruders, via experiments and numerical simulations. By varying the intruder material, we show the ability to alter the propagating wave front characteristics. Experiments agree well with discrete particle simulations.

Granular crystals are materials composed of ordered arrangements of particles in contact with each other, characterized by a highly nonlinear dynamic response. The transient dynamic response of one-dimensional highly nonlinear (uncompressed) granular crystals has been studied extensively[1,2], however few reports have explored wave propagation in two-dimensional systems[3]. The present work investigates the propagation of stress waves, or acoustic waves, in highly nonlinear two-dimensional granular crystals composed of a squared array of steel spheres and interstitial cylindrical intruders (Figure 1). Specifically, we analyze the influence of underlying particle composition on the wave front shape. We report that it is possible to substantially alter the shape of the wave front traveling through the system after impulsive loading by methodically varying the intruder material. These findings could lead to the development of new shock protecting materials and acoustic filters.

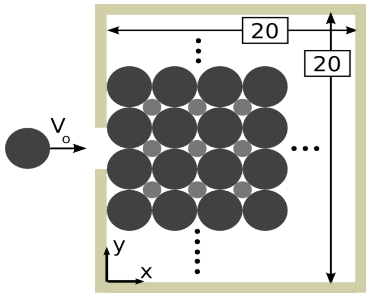

Figure 1 Schematic diagram of the experimental setup.

Numerical simulations were performed using a discrete particle model, in which each sphere or cylinder is modeled as a point mass connected by nonlinear springs. Hertzian potential[4] is used to model the sphere-sphere and sphere-wall interactions and a similar potential[5] is used to model the sphere-cylinder force displacement relation. Dissipative terms, such as friction, were not included in the simulations. Material properties chosen for the simulations are given in Table 1.

Experiments were performed on self-standing crystals assembled within a confining box made of delrin-lined walls (Figure 1). The array of particles included a 20 by 20 array of large steel spheres (19.05 mm diameter) with small interstitial intruders (7.89 mm diameter and 19.05 mm height). A striker-sphere identical to the particles composing the array was used to generate stress waves between two central particles in the array. The striker velocity was recorded with an optical velocimeter just before impact, and the recorded value was used as input in the numerical simulations. Several custom-fabricated sensor particles, instrumented with calibrated miniature tri-axial accelerometers, were positioned in selected locations in the array. The recorded accelerations were then compared with the acceleration of the center of mass of each particle obtained from the numerical simulations.

Material	Mass density (kg/m^3)	Young's Modulus (GPa)	Poisson's Ratio
Stainless Steel (type 316)	8000	193	0.30
Aluminium	2740	69	0.33
Teflon (PTFE)	1200	0.5	0.46

Table 1 Material properties used in numerical simulations.

Experiments were performed on the square packing of spheres with and without the presence of the cylindrical intruders, and were shown to be in good agreement with the numerical simulations (see Figure 2, comparing experimental and simulation results for an array without intrud-

Phononics 2011: First International Conference on Phononic Crystals, Metamaterials and Optomechanics
Santa Fe, New Mexico, USA, May 29-June 2, 2011
PHONONICS-2011-0030

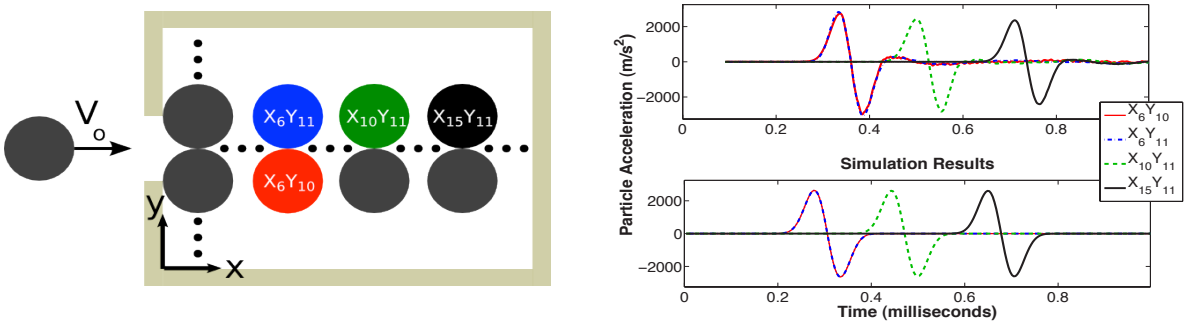

Figure 2 The left figure shows locations of sensor particles in the experimental setup (V_o = 0.29 m/s). The right figure compares experimental results (top right) with the simulation results (bottom right) for each of the sensor locations.

ers). In the absence of cylindrical intruders, the crystal was shown to support the propagation of solitary waves with comparable properties to the solitary waves previously observed in one-dimensional systems[1,2].

Numerical simulations showed the ability to significantly alter the stress wave front by introducing indruder particles of variable materials. A crystal composed of a squared array of particles without intruders supports the formation and propagation of highly nonlinear solitary waves along the two central chains (in line with the impact direction) and along the side of the crystal (following a quasi one-dimensional behavior, see Figure 3a). However, when cylindrical intruders were included the shape of the wavefront was observed to vary. When Teflon cylinders were used as intruders (Figure 3b) the wave front remained highly directional, similar to the case where intruders are absent, but the initial pulse begins to spread and shed energy in trailing pulses. The use of aluminium intruders allowed spreading of the wavefront into a triangular pattern (Figure 3c). Finally, when stainless steel intruders were used, we observed a nearly circular wavefront (Figure 3d) with particle velocities distributed over a larger area of the crystal. The ability to control the stress wave properties in these granular cystals may allow for the development of new wave-tailoring materials which could be used, for example, as protective layers capable of redirecting and trapping impact energy.

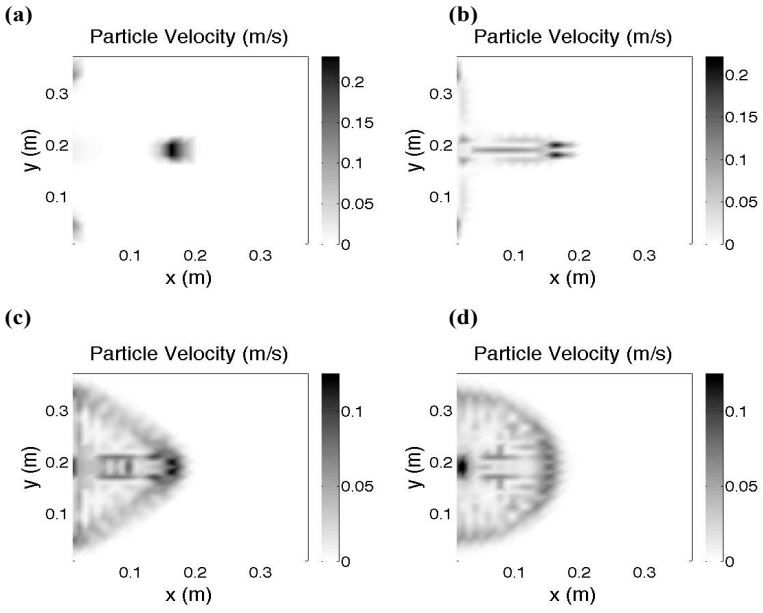

Figure 3 Numerical results showing the wave front shape in terms of particle velocity magnitude at simulation time 0.35 ms after the striker impact (V_o = 0.6 m/s) for test configurations composed of steel spheres in a square packing with **(a)** no intruders **(b)** PTFE intruders **(c)** aluminium intruders and **(d)** steel intruders.

This work was supported by the DOE SCGF and the Army Research Office MURI (Dr. David Stepp).

References

[1] V.F. Nesterenko, *Dynamics of Heterogeneous Materials*, Springer, USA (2001).
[2] C. Coste, E. Falcon, and S. Fauve, *Phys. Rev. E* **56,** (1997).
[3] A. Shukla, C.Y. Zhu, and M. Sadd, *Journal of Strain Analysis* **23**, (1988).
[4] K.L. Johnson, *Contact Mechanics*, Cambridge University Press, USA (1985).
[5] M. J. Puttock and E. G. Thwaite, *National Standard Laboratory Technical Paper No.25*, CSIRO, Australia (1969).

Phononics 2011: First International Conference on Phononic Crystals, Metamaterials and Optomechanics
Santa Fe, New Mexico, USA, May 29-June 2, 2011
PHONONICS-2011-0031

Active Control of Band Gaps by Periodically Distributed Piezo-shunts

S. B. Chen , J. H. Wen, G. Wang, D. L. Yu, X. S. Wen

Institute of Mechatronical Engineering, National University of Defense Technology, Changsha 410073, China, csbuniversity.student@sina.com, wenxs@vip.sina.com

Abstract: Periodic arrays of inductive or negative capacitive shunted piezoelectric patches are employed to control the band gaps of phononic beams. An epoxy beam with periodically surface-bonded piezoelectric patches is designed. The band gaps, when each piezo-patch is connected to a single inductive or negative capacitive circuit, are investigated in detail.

In the last decades, extensive efforts have been exerted to analyse the propagation of elastic or acoustic waves in periodic composite materials called phononic crystals[1-3]. A lot of work is particularly focused on the characteristics of so-called phononic band gaps, in which elastic wave propagation is completely blocked. These are referred to as stop bands or band gaps. The development of smart materials used to design intelligent phononic crystals whose spectral width and band gap location can be actively tuned has received considerable attention[4-10].

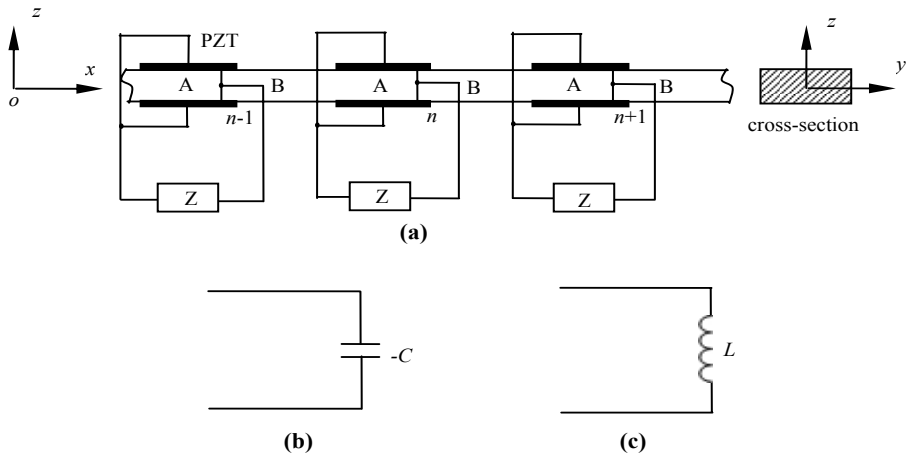

Figure 1 Phononic beam with negative capacitive or inductive piezo-shunts; **(a)** Schematic diagram of the configuration; **(b)** Negative capacitive shunting circuit. **(c)** Inductive shunting circuit.

Periodic arrays of inductive or negative capacitive shunted piezoelectric patches are employed to control the band gaps of phononic beams. An epoxy beam with periodically surface-bonded piezoelectric patches is designed, as shown in Figure 1. Each piezoelectric patch is connected to a single, independent inductive or negative capacitive circuit.

The location and the extent of induced band gaps depend on the mismatch in impedance genera-ted by each patch. The total impedance mismatch is deter-mined by the added mass and stiffness of each patch as well as the shunting electrical impedance. Therefore, the band gaps of the shunted phononic beam can be actively tuned by properly selecting the parameters of shunting circuits.

The shunting inductance combining with the intrinsic capacitance of piezoelectric patch constitutes an oscillator, which interacts with the matrix beam through electromechanical coupling effect. In analogy to locally resonant structures with mechanical vibrators, the beam with periodic inductive-shunts can form a locally resonant gap in it as well, which is closely related to the eigenfrequency of the resonant shunts. The eigenfrequency of the inductive shunting circuit can be expressed as

$$f = \frac{1}{2\pi\sqrt{LC_p}} \tag{1}$$

Phononics 2011: First International Conference on Phononic Crystals, Metamaterials and Optomechanics
Santa Fe, New Mexico, USA, May 29-June 2, 2011
PHONONICS-2011-0031

where C_p is the inherent capacitance of piezoelectric patches. However, the locally resonant gap induced by inductive shunts is not completely identical with the conventional locally resonant gap induced by mechanical vibrators in that the eigenfrequency of former type is out of the band gap, while the latter is in.

Different from the inductive shunts, the negative capacitive shunts are used to tune the Bragg gaps of the beam, because there is no local resonance in the shunting circuits. Nevertheless, the negative capacitive shunts can effectively increase the electromechanical coupling factor of the piezo-patches and modify the equivalent modulus of the elements bonded with piezo-patches in the beam, which can be given by

$$E_{\mathrm{p}} = \frac{h_p\left(C_p - C\right)}{h_p s_{11}^E\left(C_p - C\right) - {d_{31}}^2 A_s} \tag{2}$$

where s_{11}^E is the piezoelectric material's compliance coefficient at constant electric field intensity. d_{31} is the piezoelectric constant that couples the mechanical and electrical properties of the piezoelectric material. A_s is the area of electrodes. h_p is the thickness of piezoelectric patch. Contrary to inductive shunts which are passive circuits, the negative capacitive shunts are active circuits that have external energy input, so the proposed approach will be afflicted by instability problems[11,12]. To avert the system being destabilized by negative capacitive shunts, the stable conditions of the shunting system are investigated in detail.

Control of the band gaps of phononic beam with piezo-shunts is demonstrated numerically, employing transfer matrix method with periodic boundary conditions and the Bolch theorem. The variations of band gaps with different shunting parameters are discussed in the paper, subsequently. The result reveals that inductive shunts can induce local resonances in the beam and form locally resonant gaps around the eigenfrequency, but negative capacitive shunts can tune the Bragg gaps readily and effectively. The theoretical results are verified with commercial finite element software by calculating transmission properties of finite periods. Because negative capacitive shunted phononic beam are a non-conservative system with external energy input, the stability conditions are investigated in this paper. The result reveals that the stability can be judged readily by the value of equivalent modulus of the elements bonded with piezo-patches. Though negative modulus will occur in both inductive and negative capacitive shunting systems, the inductive shunting system is a conservative system which is stable, because its negative modulus is a dynamic value and frequency dependent, while the negative capacitive shunting system will become unstable, if the equivalent modulus becomes negative, which is a static value and frequency independent.

References

[1] D. J. Mead, *J. Sound Vib.* **11**, 181-197 (1970)
[2] D. J. Mead and S. Markus, *J. Sound Vib.* **90**, 1-24 (1983)
[3] M. S. Kushwaha, P. Halevi and L. Dobrzynski, *Phys. Lett. A* **71**,2022-2025 (1993)
[4] M. Ruzzene and A. Baz, *Proc. SPIE* **3991**, 389-407 (2000)
[5] A. Baz *J. Vibration and Acoustics*. **123**, 472-479 (2001)
[6] O. Thorp, M. Ruzzene and A. Baz, *Proc. of SPIE* **4331,** 218-238 (2001)
[7] O. Thorp, M. Ruzzene and A. Baz, *Smart Mater. Struct.* **14,** 594-604 (2005)
[8] A. Spadoni, M. Ruzzene and K. A. Cunefare, *J. Intell. Mater. Syst. Struct.* **20,** 979-90 (2009)
[9] F. Casadei, M. Ruzzene, L. Dozio and K. A. Cunefare, *Smart Mater. Struct.* **19,** 015002 (2010)
[10] S. B. Chen, X. Y. Han, D. L. Yu and J. H. Wen, *Acta Phys. Sin.* **59,** 387-392 (2010)
[11] S. Behrens, A. J. Fleming and S. O. R. Moheimani, *Smart Mater. Struct.* **12**, 18-28 (2003)
[12] B. de Marneffe and A. Preumont, *Smart Mater. Struct.* **17**, 035015 (2008)

Phononics 2011: First International Conference on Phononic Crystals, Metamaterials and Optomechanics
Santa Fe, New Mexico, USA, May 29-June 2, 2011
PHONONICS-2011-0041

The Role of Array Symmetry in the Transmission of Ultrasound through Periodically Perforated Plates

H. Estrada[1,2], P. Candelas[1], F. Belmar[1], A. Uris[1], V. Gómez[1], F. J. García de Abajo[3], F. Meseguer[1,2]

[1]Centro de Tecnologías Físicas, Unidad Asociada ICMM–CSIC/UPV, Universidad Politécnica de Valencia, Av. de los Naranjos s/n. 46022 Valencia, Spain
hector.estrada@icmm.csic.es, pcandelas@fis.upv.es, fbelmar@fis.upv.es, auris@fis.upv.es, vgomez@fis.upv.es, fmese@fis.upv.es
[2]Instituto de Ciencia de Materiales de Madrid (CSIC), Cantoblanco, 28049 Madrid, Spain
[3]Instituto de Óptica - CSIC, Serrano 121, 28006 Madrid, Spain
J.G.deAbajo@csic.es

Abstract: We present angle-resolved experimental results on the role of array symmetry in the transmission features of periodically perforated plates. A very rich interplay between Fabry-Perot single-hole resonances, coherent scattering and plate vibration is found. By comparing several spatial hole arrangements, the effects of the geometry are disentangled from the contribution of plate vibrations.

The study of periodic structures interacting with sound can be tracked back to the end of the 19th century with the work of Rayleigh[1], who studied the reflection coefficient of a one dimensional grating. Later, in 1953, Brillouin[2] attempted a unification of the concepts involved in the behavior of electromagnetic and mechanical waves in periodic media. More recently, the propagation of electromagnetic waves through metallic membranes perforated with subwavelength periodic hole arrays has received considerable attention. Experiments[3] have showed that at certain frequencies strongly correlated with the array period, light transmission per hole is higher than predicted for non-interacting holes theory[4]. These ideas, originally developed in the context of electromagnetic waves, have been transferred to acoustic waves[5-8] and this phenomenon is now known as Extraordinary Acoustic Transmission (EAT), although it has been recently demonstrated[9] that for the acoustic case there is not as extraordinary as in optics. Fabry-Perot resonances in the holes produce the main contribution to the full transmission peaks.

Our experimental setup is based on the well-known ultrasonic immersion technique. The plate is placed between the ultrasonic transducers (around 250 kHz) in a water tank. Measurements of transient signal are averaged over 100 runs. The plate is then rotated to obtain the dependence on the parallel-to-the-plate wave-vector (see Fig. 1). The transmission spectrum is normalized with the spectrum measured without the plate. The plate thickness is 2 mm and more than 1500 holes of 3 mm in diameter were drilled in aluminum and brass plates having different array geometries such as square, rectangular, triangular, and pseudo random. Transmission dispersion for these different array arrangements are shown in Fig. 2. The sound line does not correspond to the line where the data ends because our experimental setup cannot be used to measure plate rotation angles above 60º. In agreement with previous results[8,10] , a very rich interplay between hole resonances, coherent interference, and plate modes is observed in Fig. 2 **(a)**, **(b)**, and **(d)**. However, when the translational symmetry is broken by drilling the holes in a pseudo-random manner (Fig. 2**(c)**), the transmission dispersion becomes smoother. This allow us to identify the contribution of the perforated plate vibration, which can be seen as a minimum corresponding to a leaky surface mode.

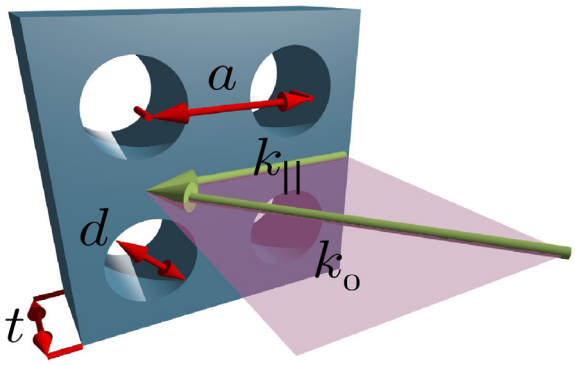

Figure 1 Scheme of the geometry for the transmission of ultrasound through perforated plates. An incident wave having wave-vector k_0 arrives at the plate of thickness t, which is perforated with holes of diameter d and period a. The parallel to the plate component of the incident wave-vector $k||$ is varied by rotating the plate with respect to the source.

Phononics 2011: First International Conference on Phononic Crystals, Metamaterials and Optomechanics
Santa Fe, New Mexico, USA, May 29-June 2, 2011
PHONONICS-2011-0041

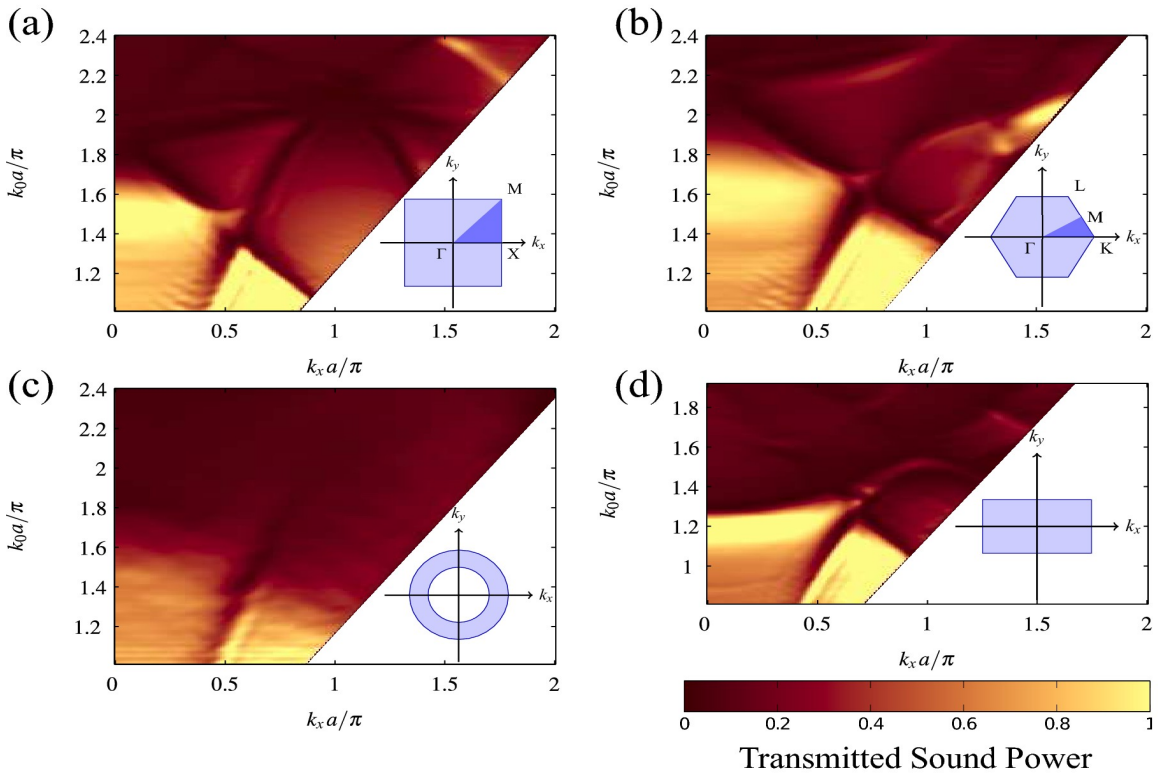

Figure 2 Transmitted sound power measured at ultrasonic frequencies for perforated plates of thickness t=2 mm immersed in water and different array geometries. The insets show the reciprocal space of the hole arrays and their corresponding orientation relative to the first Brillouin zone. **(a)** Square array of period a=5 mm drilled in an Al plate. **(b)** Triangular array of period a=5 mm drilled in an Al plate. **(c)** Pseudo-random array having an average period a=5 mm, also drilled in an Al plate. **(d)** Rectangular array of periods a_x=4 mm, a_y=6 mm drilled in a brass plate.

Additionally, full transmission is quenched to 1/2 in the absence of coherent interference. Translational symmetry is also the key factor for the appearance of the observed dips which vary depending on the geometry. These minima arise from the hybridization of Wood anomalies[11] (i.e. lattice modes) with plate modes. Pure Wood anomaly minima can be observed if the impedance mismatch between the holey plate and the surrounding fluid is large enough to assume that the plate is perfectly rigid and the sound cannot penetrate it. The crossing between the Wood anomaly and the surface mode can be clearly seen for the three symmetric arrays. This crossing is particularly interesting because it involves the surface mode, the Wood anomaly minimum, and the transmission peak, all of them hybridized. Thus, the array symmetry plays a key role in the transmission features of perforated plates. The existence of full transmission peaks and Wood anomaly minima, both depending on coherent interference among holes, can be only guaranteed by the translational symmetry of the array.

References

[1] Lord Rayleigh. *The Theory of Sound*, Vol. II. 2nd edition, Macmillan London (1896).
[2] L. Brillouin. *Wave Propagation in Periodic Structures*. Dover New York (1953).
[3] T. W. Ebbesen, H. J. Lezec, H. F. Ghaemi, T. Thio, and P. A. Wolff, *Nature*, **391**,667–669 (1998).
[4] H. A. Bethe. *Phys. Rev.*, **66**, 163–182 (1944).
[5] Bo Hou, Jun Mei, Manzhu Ke, Weijia Wen, Zhengyou Liu, Jing Shi, and Ping Sheng, *Phys. Rev. B*, **76**, 054303 (2007).
[6] J. Christensen, L. Martin-Moreno, and F. J. Garcia-Vidal, *Phys. Rev. Lett.*, **101**, 014301 (2008).
[7] H. Estrada, P. Candelas, A. Uris, F. Belmar, F. J. García de Abajo, and F. Meseguer, *Phys. Rev. Lett.*, **101**, 084302 (2008).
[8] H. Estrada, F. J. García de Abajo, P. Candelas, A. Uris, F. Belmar, and F. Meseguer, *Phys. Rev. Lett.*, **102**, 144301 (2009).
[9] F. J. García de Abajo, H. Estrada, and F. J. Meseguer, *New J. Phys.*, **11**, 093013 (2009).
[10] H. Estrada, P. Candelas, A. Uris, F. Belmar, F. J. García de Abajo, and F. Meseguer, *Appl. Phys. Lett.*, **95**, 051906 (2009).
[11] R. W. Wood, *Phil. Mag.*, **4**, 396 (1902).

Phononics 2011: First International Conference on Phononic Crystals, Metamaterials and Optomechanics
Santa Fe, New Mexico, USA, May 29-June 2, 2011
PHONONICS-2011-0044

Phonons on Complex Networks

Guimei Zhu[1,2] and Baowen Li[1,2]

[1] *NUS Graduate School for Integrative Sciences and Engineering, Singapore 117456, Singapore,*
[2] *Department of Physics, National University of Singapore, Singapore 117542, Singapore,*
g0801859@nus.edu.sg, phylibw@nus.edu.sg

Abstract: We map the nodes and edges of complex network to oscillators and couplings between them. We thus can study the multi-scale structures of networks through the properties of eigenmodes of laplacian matrix – *the phonons on complex networks*. The phonons from low to high frequencies are used as probes of the structural characteristics from macro- to micro-scales. This characteristic can be used as a structural measure of complex networks. These findings may have potential applications in real networks, such as heat conduction on nanotube/nanowire networks and biological networks.

Introduction

Vibrational dynamics has been widely used to study thermodynamic properties of various structures in solid-state physics and/or other disciplines. Since the structure is considered as a primary factor responsible for physical properties, reaching a reliable comparison of the structure patterns at different scales in a quantitative way is of primary importance for us to know the underlying structure how the dynamic transport processes of mass, energy, signal and/or information from micro- to macro-structural scales. The effect of network structures on electronic and thermal properties has been one of the most active topics in recent years[1, 2].

Methods

In this paper, we map the nodes and the edges to oscillators and couplings between them. The *vibration modes (phonons)* are used as probes of the structural patterns. One phonon with a specific frequency is sensitive only to the structural patterns matching in size with its frequency. By using all the vibration phonons from low to high frequencies we can detect the pattern properties from macro- to micro- scales.

The topological structure of a network can be described by an adjacency matrix A. The elements A_{ij} are 1 and 0 if the nodes i and j are connected and disconnected, respectively. We map the nodes to oscillators and the edges to harmonic couplings between the connected nodes. Denoting the displacements of the oscillators with $(y_1, y_2, \ldots y_N)$ the equations governing the dynamical process of the network reads, $\mu \ddot{y}_i = k\sum_{s=1}^{N} A_{is}\left(y_s - y_i\right)$, N is the network size, μ the mass of each oscillator and k the coupling strength. For simplicity, let $k/\mu = 1$. Assuming $Y \equiv Xe^{i\omega t}$, $Y^T \equiv [y_1, y_2, \ldots y_N]$, $X^T \equiv [x_1, x_2, \ldots x_N]$, the equations can be rewritten as, $\omega^2 X = GX$, G the coupling matrix, also named Laplacian Matrix, which reads,

$$G_{ij} = \begin{cases} \sum_{i=1}^{N} A_{ij} = k_i, & (i = j) \\ -A_{ij}, & (i \neq j) \end{cases} = k_i \delta_{ij} - A_{ij}. \qquad (1)$$

The eigenvalues of G are nonnegative and can be ranked as, $0 = \lambda_1 \leq \lambda_2 \cdots \leq \lambda_N$. Assuming the network is in a thermal bath with a definite temperature, a simple computation leads to the cross-correlations between the fluctuations of the phonons,

$$\left\langle y_i \cdot y_j \right\rangle \propto \left(G^{-1}\right)_{ij} = \sum_{m=2}^{N} \left(\lambda_m^{-1} \cdot X_m X_m^T\right)_{ij}. \qquad (2)$$

Phononics 2011: First International Conference on Phononic Crystals, Metamaterials and Optomechanics
Santa Fe, New Mexico, USA, May 29-June 2, 2011
PHONONICS-2011-0044

It follows that the contribution of an individual phonon is, $G_{ij}(m) \propto \left(\lambda_m^{-1} \cdot X_m X_m^T\right)_{ij}$. The phonons with small values of λ_i , the corresponding motions are collective and global, and can measure the characteristics of macro-scale patterns. The phonons with large values of λ_i, on the other hand, describe uncorrelated motions occurring in different micro-scale regions, which are sensitive to micro-scale patterns. Hence, the phonons can detect the structural patterns from macro- to micro-scales.

Results:

Figure 1 demonstrates that a phonon with a specific frequency is sensitive only to the structural patterns matching in size with its frequency.

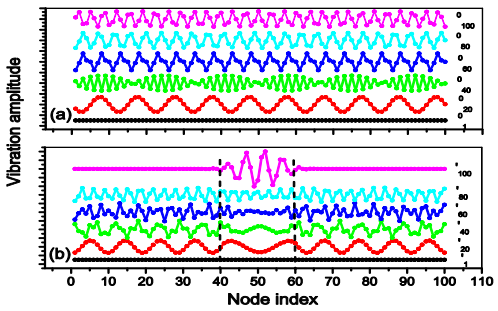

Figure 1 phonons on networks can be used as probes of structural patterns at different scales. (a) A circular network is constructed by connecting each nodes with its nearest four neighbors. The sizes is N=100. On this regular network, the phonons are periodic waves. The wavelength is measured in unite of the lattice size. (b) A densely connected deformation is constructed in the segment 40-60 by connecting each node in this region with its six nearest neighbors (instead of the originally four nearest neighbors). Phonons with comparatively large wavelenghths keep unchanged or deform slightly, while phonons matching with the deformation(e.g., λ'_{100}) become localized in the deformation region

We have applied the method to the Santa Fe Institute collaboration network[3]. We first normalize the components of the phonons, namely, $X_i^s = | X_i / \max(X_i) |,\ i = 1, 2, \cdots, N.$ Then a threshold τ^s can be used to identify the nodes involved in the phonons, respectively. The nodes with large values of component X_i^s ($\geq \tau^s$) are regarded as the nodes involved in the corresponding phonons. For each phonon, the components of the nodes involved in it are distinguishably large compared with that of the others. Hence, the τ^s -based results are robustness. In the present work, we choose the $\tau^s = 0.1$. The detail results are shown in Fig 2 (details can be seen from Ref [4]).

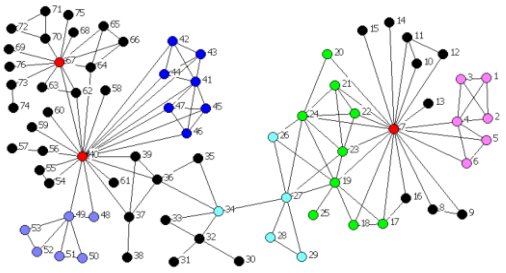

Figure 2 A part of largest component of the Santa Fe Institute collaboration network. There are totally 76 nodes. The phonons $\lambda_{76}, \lambda_{75}$ *and* λ_{74} can detect the three hubs 40, 7 and 67, marked with red color. The phonon. λ_{73} involves nodes 17 ~ 25 (green nodes), while the phonon λ_{72} covers the nodes 26 ~29 and 34 also (green and cyan). The three clusters 41 ~47 (blue), 1 ~ 6 (magenta), and 48 ~ 53 (violet), correspond to the phonons $\lambda_{70}, \lambda_{69}$ and λ_{68}, respectively.

Conclusions

To summarize, we have used the *phonon* to detect the structural patterns at different scales in model network and Santa Fe institute collaboration network. Because the phonons are sensitive only to the structural patterns matching in size with their wavelengths, the phonon from high to low frequencies can capture the pattern characteristics in a coarse-grain way.

References:

1 G. Zhu, H. Yang, C. Yin, B. Li, *Physical Review E* **77**, 066113 (2008).
2 H. J. Yang, C. Y. Yin, G. M. Zhu, B. Li, *Physical Review E* **77**, 045101 (2008).
3 M. Girvan and M. E. J. Newman, *Proceedings of the National Academy of Sciences of the United States of America* **99**, 7821 (2002).
4 G. Zhu, H. Yang, J. Ren, B. Li, *to be published.*

Phononics 2011: First International Conference on Phononic Crystals, Metamaterials and Optomechanics
Santa Fe, New Mexico, USA, May 29-June 2, 2011
PHONONICS-2011-0055

Optimal Design of Nonlinear Wave Devices

Jakob S. Jensen

Department of Mechanical Engineering, Technical University of Denmark
Nils Koppels Allé, Building 404, DK-2800 Kgs. Lyngby, Denmark
jsj@mek.dtu.dk

Abstract: The method of topology optimization is applied to wave propagation problems with nonlinearities. In the general case the iterative design procedure should be based on transient simulation of the wave propagation, but in the special case of non-instantaneous nonlinearities a steady-state optimization formulation can be applied. The latter case is exemplified by the design of a 1D optical diode.

Topology optimization has within the last decade been used successfully to design bandgap materials and devices. A gradient-based material distribution method is used to design photonic crystals with maximized bandgaps[1] and later a similar method was applied to design phononic crystals[2] and finite structures and devices with bandgap properties[2-4].

In this work we aim to extend the use of gradient-based material distribution methods to deal with wave devices that display nonlinear behavior. As is well known, the presence of nonlinearities can significantly alter the behavior of bandgap materials and structures, but can also be used to create devices with novel functionality that cannot be accomplished with a pure linear behavior.

In the general case the presence of nonlinearities generates higher order harmonics in the response and transient simulations are thus needed for the analysis of the device performance.

Steady-state model with a non-instantaneous nonlinearity
However, in certain cases it may be relevant to study a steady-state model of the nonlinear wave propagation problem. Such a model may arise if we consider a non-instantaneous nonlinearity such as e.g. in nonlinear optics with a dielectric permittivity that depends on the time-averaged intensity of the electric field.

By treating the nonlinear wave propagation problem in a steady-state framework we can reduce the computational requirements considerably. The general nonlinear model is written as follows

$$\nabla \cdot (A(u)\nabla u) + B(u)k^2 u = 0 \tag{1}$$

in which A and B are two material coefficients that depend on the local field intensity and k is the wavenumber.

Equation (1) can conveniently be solved using a standard finite element method combined with a complex incremental Newton-Raphson procedure[4]. In addition design sensitivity analysis can be performed for the finite element model using the adjoint method[4].

Example: one-dimensional optical diode
As an application example we demonstrate the design of an optical diode[5]. Ideally, the diode allows for undisturbed transmission in one direction whereas the propagation in the opposite direction is hindered. As objective for the optimization we choose to maximize the difference in transmission in the two opposing directions and thereby create a diode-like performance of the device. The optimization problem is illustrated in Figure 1(**a**).

In the device we aim to distribute two materials, a linear dielectric material with the relative permittivity $\varepsilon_r=1$ and a nonlinear material with relative permittivity $\varepsilon_r=\varepsilon(1+\gamma|e|^2)$, in which ε is the linear permittivity of the material, $|e|^2$ is the intensity of the electric field and γ is a nonlinear parameter. The permittivity in each finite element in the discretized model is governed by a single continuous design variable. The optimized set of design variables is found with an iterative gradient-based procedure using the method of

Phononics 2011: First International Conference on Phononic Crystals, Metamaterials and Optomechanics
Santa Fe, New Mexico, USA, May 29-June 2, 2011
PHONONICS-2011-0055

moving asymptotes[6].

Figure 1(**b**) shows a specific optimized design obtained for ε=1.1 and γ=0.1. Plotted in the figure are the values of the continuous design variable for each finite element with the value 0 corresponding to the linear material and the value 1 corresponding to the nonlinear material. It is seen that the optimized design consists of alternating sections of nonlinear and linear dielectric material. Figure 1(**c**) shows the magnitude of the effective permittivity for waves propagating in opposing directions, indicating the large difference in material properties which is obtained.

As a result of the material distribution a difference in transmission in the two opposing propagation direction of about 10 percent is noted. However, larger differences can be obtained if the structure is longer compared to the wavelength.

The results for the 1D diode was supplemented with an optimization study for a 2D waveguide that displays a transmission that is a highly nonlinear function of the input intensity[5]. Currently, the diode example is being re-investigated using a transient formulation including an investigation of design of an optical switch. Additionally, the transient problem is being implemented for mechanics problems as well.

References

[1] S. J. Cox and D. C. Dobson, *SIAM J. Appl. Math.* **59**, 2108-2120 (1999).
[2] O. Sigmund and J. S. Jensen, *Phil. Trans. R. Soc. Lond. A* **92**, 1001-1019 (2003).
[3] M. I. Hussein, K. Hamza, G. M. Hulbert, and K. Saitou, *Waves in Random and Complex Media* **17**, 491–510 (2007).
[4] C. J. Rupp, A. Evgrafov, K. Maute, and M. L. Dunn, *Structural and Multidisciplinary Optimization* **34**, 111–121 (2007).
[5] J. S. Jensen, submitted (2011).
[6] K. Svanberg, *Int. J. Numer. Methods Eng.* **24**, 359–373 (1987).

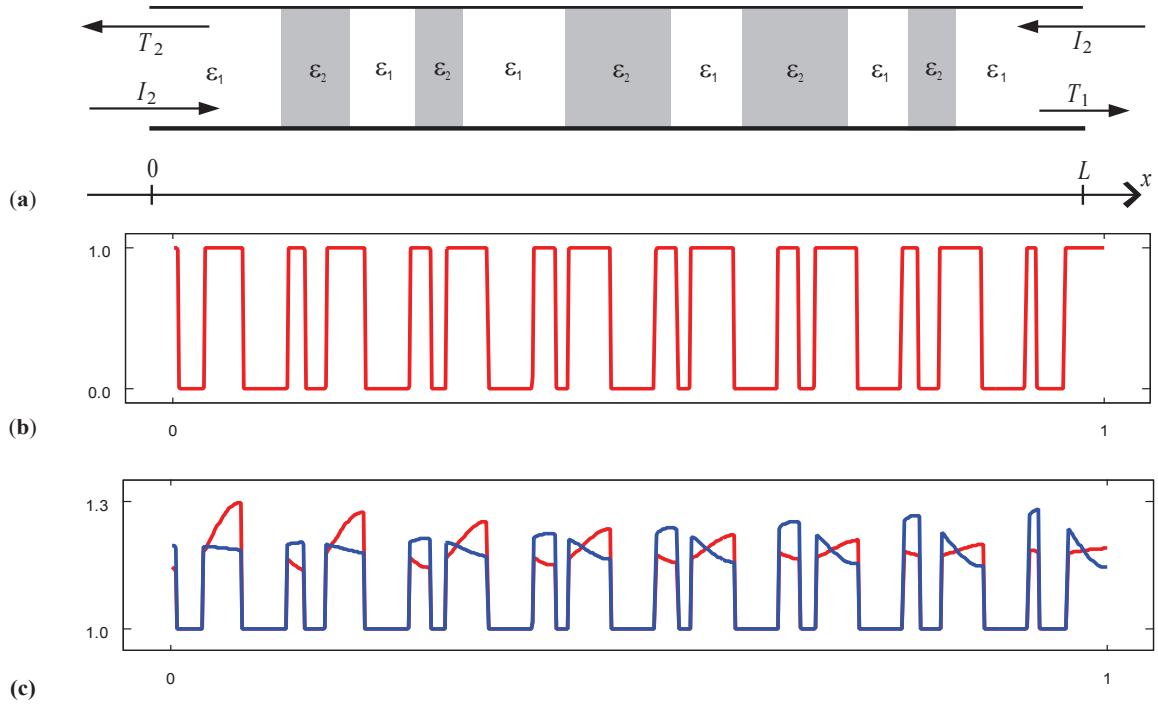

Figure 1 Example of an optimized 1D nonlinear wave device. (**a**) Design problem: the difference in transmission of incoming waves from opposing directions is maximized by distribution a linear dielectric material ε_1 and a nonlinear dielectric material ε_2, (**b**) the resulting design illustrated by the elementwise optimized values of the design variable (0 is linear and 1 is nonlinear), (**c**) the effective material permittivity in the structure when the wave propgates towards right (red line) and towards left (blue line).

Phononics 2011: First International Conference on Phononic Crystals, Metamaterials and Optomechanics
Santa Fe, New Mexico, USA, May 29-June 2, 2011
PHONONICS-2011-0057

EFIT Simulation of Ultrasonic Wave Propagation in Complex Microfluidic Structures

M. Zubtsov[1], R. Grundman[1], R. Lucklum[1]

[1] *Institute of Micro and Sensor Systems, Otto-von-Guericke-University, Magdeburg, Germany*
mikhail.zubtsov@ovgu.de, ralf.lucklum@ovgu.de

Abstract: The Elastodynamic Finite Integration Technique (EFIT) is used to simulate ultrasonic wave propagation in complex microfluidic structures comprising fluidic channels, phononic crystal structures and piezoelectric transducers. An EFIT computational math is combined with MATLAB coding. The viability of the approach is demonstrated.

The precise spatial and temporal control afforded by microfluidic devices make them uniquely suited to solve many challenging problems in sample treatment and analysis at micro and nano scales. Dealing with the dynamics and engineering of fluids confined on the micrometer scale microfluidics involves the large number of different basic phenomena and a combination of a broad variety of effects and means including ultrasound, which has shown to be a viable technique for some microfluidic tasks like microparticles manipulation, stirring, mixing and streaming of microvolumes [1] as well as characterization. Phononic crystal devices may significantly expand the use of ultrasound in microfluidic systems, since they offer a wide range of functionalities [2, 3], which can be beneficially utilized to improve microfluidic system operation and enable new applications.

However, in order to integrate this new class of acoustically active and reactive devices into existing liquid manipulation units, an analysis of the total acoustic field is required. There is an apparent need for a better understanding of interactions between ultrasonic waves and complex structures comprising both active and reactive components. We consider an EFIT, which relies on the direct discretization of the Newton-Cauchy's equation of motion and the equation of deformation rate, and where all field quantities are function of position and time, as a proper math ground for an efficient simulation tools which can solve this problem.

The EFIT starts with the elastodynamic governing equations in integral form and simulates the ultrasonic wave field without any approximations. Using unique discretization of the basic field equations on a staggered grid the method permits to implement a pertinent code for widely arbitrary inhomogeneous composites [4]. In general, the FIT also permits a unified treatment of the acoustic, electromagnetic, elastodynamic and piezoelectric cases [5]. In all these instances, the underlying governing equations in integral form are discretized on the same a dual grid complex in space and time, which yields the so-called discrete grid equations. Another advantage of the FIT approach is that the resulting discrete matrix equations represent a consistent one-to-one translation of the underlying field equations. The use of discrete topological operators ensures important vector analytical properties in the discrete grid space.

The FIT implicitly insures that the numerical results are free of late-time instabilities and artificial sources. On account of the complexity of multiple acoustically active and reactive units including PZT devices integrated into a single structure we consider this unified approach as the most appropriate to the problem, in particular, taking into account simplicity of the FIT, which allows an easy and efficient implementation on various computer architectures.

Phononics 2011: First International Conference on Phononic Crystals, Metamaterials and Optomechanics
Santa Fe, New Mexico, USA, May 29-June 2, 2011
PHONONICS-2011-0057

A regularly perforated wall between two parallel and adjacent fluidic channels has been used as the first test sample to evaluate applicability of the method. This model represents one of possible setups of phononic crystal sensor integrated into a microfluidic system. The EFIT-code and other relevant routines are implemented with MATLAB which provides a user interface and different output opportunities that help to analyze and visualize the simulation results. The possibility of parallel computing to afford bigger and/or more detailed models has also been realized.

A good agreement between the first EFIT results and similar simulations using COMSOL Multiphysics™ and FTDT has been demonstrated. Basic simulations we have performed show all the kind of interactions between propagating wave and the structure, which are typical for an acoustic-structure interaction,

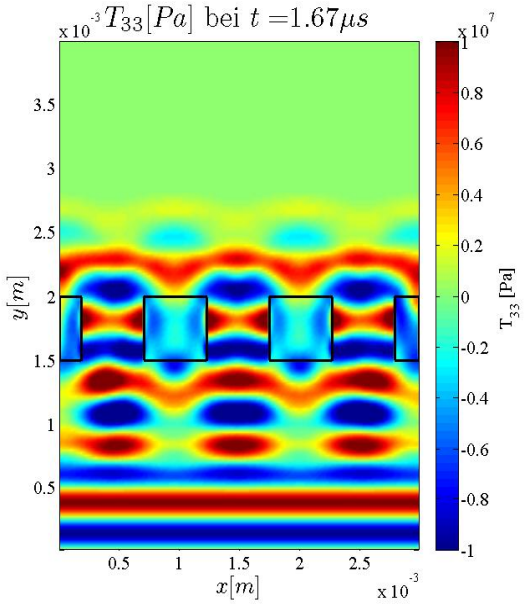

Figure 1 Spatial distribution of T_{33} field in the diffraction of plane wave at subwavelength regime. Perforation periodicity **a**=1 mm, the wavelength **λ**=**a**, and the size of the perforation **b**=**a**/2.

including those which are not available in semi-analytic methods. Some are illustrated on the Fig.1. This presents a time-domain snapshot of a time-harmonic acoustic plane wave impinging on an infinite and regularly perforated quasi-1D plate. This particular setup, specifically, diffraction of emanating from the wall of fluidic channel plane wave and impinging on regularly perforated intermediate wall at the subwavelength regime, relates to one of possible sensing applications. Namely, we consider presented here effects of mode conversion as well as effects which are coupled with the resonant propagation through the plate as good candidates that may afford a distinctive measurand feature.

References

[1] T. Torii, *Advances in Biochemical Engineering-Biotechnology*, **119**, 165-177 (2010).
[2] R. H. Olsson III and I. El-Kady, *Meas. Sci. Technol*., **20** (2008).
[3] Sz-Chin Steven Lin et al., *Phys. Rev*. B **79**, 094302 (2009).
[4] R. Marklein, *Numerical Methods for the Modeling of Acoustic, Electromagnetic, Elastic and Piezoelectric Wave Propagation Problems in the Time Domain Based on the Finite Integration Technique*, Shaker Verlag, Aachen, (1997).
[5] R. Marklein, *The Finite Integration Technique as a General Tool to Compute Acoustic, Electromagnetic, Elastodynamic, and Coupled Wave Fields*, in W. R. Stone (ed.), Review of Radio Science, 1999-2002 URSI, IEEE Press and John Wiley and Sons, pp. 201-244 (2002).

Phononics 2011: First International Conference on Phononic Crystals, Metamaterials and Optomechanics
Santa Fe, New Mexico, USA, May 29-June 2, 2011
PHONONICS-2011-0058

Acoustic Beams in Finite Sonic Crystals

V. Romero-García[1,4], R. Picó[2], V. Sánchez-Morcillo[2], L.M. Garcia-Raffi[3], J.V. Sánchez-Pérez[4], K. Staliunas[5]

[1] *Instituto de Ciencia de Materiales de Madrid, Consejo Superior de Investigaciones Científicas, Spain*
virogar1@gmail.com,
[2] *Instituto de Investigación para la Gestión Integrada de zonas Costeras, Universidad Politécnica de Valencia, Spain*
rpico@fis.upv.es, victorsm@upv.es,
[3] *Instituto Universitario de Matemática Pura y Aplicada, Universidad Politécnica de Valencia, Spain*
lmgarcia@mat.upv.es
[4] *Centro de Tecnologías Físicas: A.M.A, Universidad Politécnica de Valencia, Spain,*
virogar1@gmail.com, jusanc@fis.upv.es
[5] *Departament de Fisica i Enginyeria Nuclear, Universitat Politecnica de Catalunya (UPC), Spain*
kestutis.staliunas@icrea.es

Abstract: The physical properties of 2D finite periodic arrays are explored using acoustic beams with finite spatial width. Multiple Scattering Theory and the Plane Wave Expansion Method are used to study the differences between the approximation of infinite periodic medium and the finite case. In the most experimental cases the physical properties of the system are constrained by both the size of the sample and the width of the acoustic beam.

A Sonic Crystal is a periodic arrangement of cylindrical inclusions embedded in a homogeneous host material. The host material may be solid, the term Phononic Crystal is used in this case. For many applications usually these scatterers can be considered as infinitely rigid and the propagation inside them is not possible. Sonic Crystals can be designed in order to guide the acoustic energy in an appropriate way to present particular effects like focalization, auto-collimation or filtering.

The propagation of acoustic waves in a 2D periodic media can be described from its dispersion relation and the iso-frequency contours. Band gaps and propagation curves describe the propagation features for a specific direction in an infinite crystal. However, the sonic crystal is composed by a finite number of scatterers and thus, its finite size must be taken into account. The theoretical approach for a 2D finite period array is more complicated. If the beam is wide enough to be comparable to the size of the crystal at the front interface, the edge effects may become important and they cannot be neglected. It is the same case at opposite case: extremely narrow beams (comparable to the period of the crystal) do not propagate though the crystal as plane waves in a periodic medium. In the field acoustics, little attention has been paid to investigate how the finitude of the beam and the size of the sample may affect wave propagation through and outside the crystal.

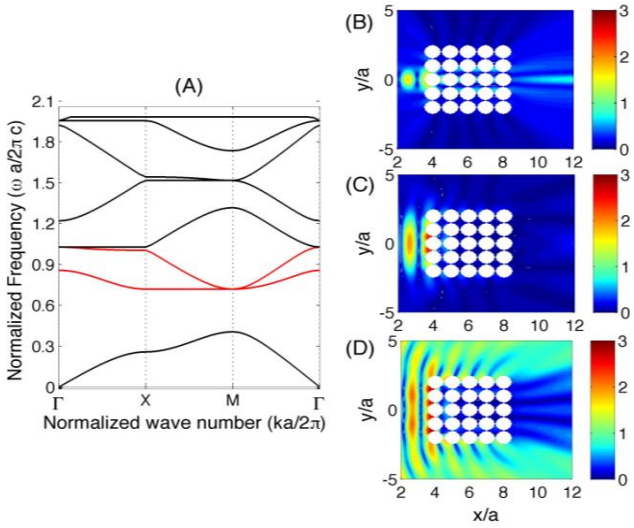

Figure 1 (A) Acoustic Band Structure of a Sonic Crystal with square periodicity (r=1m, a=0.4545). Beam propagation trhough the crystal for different beam widths (B) s=0.5, (C) s=2, and (D) s=1000 (plane wave) at f=170Hz

Multiple Scattering Theory[1] (MST) is used to solve the scattering problem of a **finite** width beam produced by the array of scatterers. A distribution of 5x5 infinite straight cylinders with radius a=0.4545 and separated r=1 (normalized units), parallel to the *z*-axis are located at (R_i, θ_i) of diameters D_i with

Phononics 2011: First International Conference on Phononic Crystals, Metamaterials and Optomechanics
Santa Fe, New Mexico, USA, May 29-June 2, 2011
PHONONICS-2011-0058

i=1, *2*, …, *N.* to form a regular square array perpendicular to the *x*-*y* plane. The total pressure in the point (*x*,*y*) is

$$P(x,y) = e^{ikx} e^{\frac{-y}{\sigma}} + \sum_{l=1}^{N} \sum_{s=-\infty}^{\infty} A_{ls} H_s(kr_l) e^{is\theta_l} \qquad (1)$$

where A_{ls} are determined by the solution of the system of equations obtained by MST, r_l and θ_l are the polar coordinates of the measuring point respect to the *l*–th scatterer and σ determines the width of the beam.

The transmission properties of the crystal are evaluated using MST. Figure 1A shows the band structure of the SC obtained using the plane wave expansion[2]. For a frequency lying in the Band Gap Figures 1B,1C and 1D show the transmission of beams with different sizes impinging at the left side of the crystal. The attenuation is optimized if the width of the beam is similar to the size of the sample.

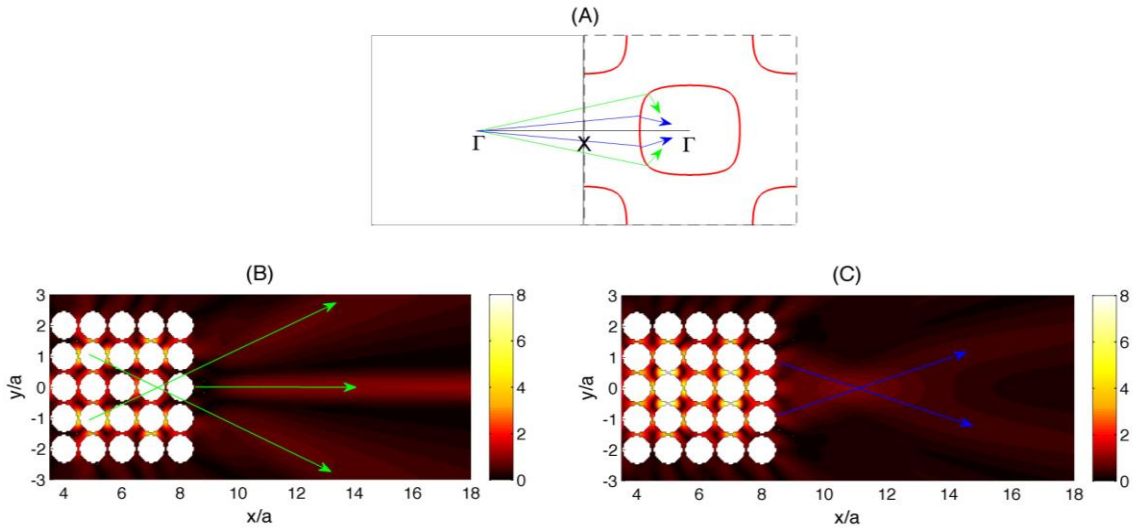

Figure 2. (A) Iso-frequency contours of the Bloch modes for the same SC as in Figure 1. The curves correspond to f=270Hz (second and third bands, in red in Figure 1A). Blue and green lines represent the projection on the curves of the spatial components of a wide and narrow beam respectively. Beam propagation behind the crystal for (B) a narrow beam (s=0.5) and (C) a plane wave (s =1000).

For wider beams (Figure 1D), the diffraction effect at the edges becomes important. The propagation of waves around the sample increases the total sound field behind the crystal. In the case of very narrow beams (Figure 1B), the propagation through the crystal is like in a homogeneous medium. In this case, the beam is not impinging the scatterers, and despite the frequency corresponds to the bandgap, it propagates through the crystal with a very low attenuation.

Special phenomena like focalization induced by propagation in a periodic medium may be significantly altered if the size of the beam is considered. For very narrow beams (Figure 2B) the Sonic Crystal in the second and third bands splits into three beams. Besides, for a beam as wide as the sample (Figure 2C) the focalization is produced some periods behind the crystal.

References

[1] P.A. Martin, *Multiple Scattering: Interaction of Time-Harmonic Waves with N Obstacles*, Cambridge University Press, UK (2006).
[2] M.S. Kushwaha, P. Halevi, G Martínez, L dobrynski and Djafari-Rouhani. *Phys. Rev. B* **49**, (4) 2313 (1994).

Phononics 2011: First International Conference on Phononic Crystals, Metamaterials and Optomechanics
Santa Fe, New Mexico, USA, May 29-June 2, 2011
PHONONICS-2011-0067

Broadband Vibration Attenuation Induced by Periodic Arrays of Feedback Shunted Piezoelectric Patches on Beams

Gang Wang, Shengbing Chen, Jihong Wen

Institute of Mechatronical Engineering, National University of Defense Technology, Changsha, China
and the Key Laboratory of Photonic and Phononic Crystal, Ministry of Education, China
wg.nudt@gmail.com

Abstract: The effect of periodic arrays of feedback shunted piezoelectric patches in vibration attenuation of flexible beams is analyzed theoretically and experimentally. Broadband vibration attenuations are observed no mater in or out of the band gaps. The proposed concept is validated experimentally on a suspended epoxy beam.

The present work involves a feedback shunting strategy in the phononic crystals (PCs) composed of periodic array of shunted PZT patches and a flexible beam for the broadband attenuation of vibration. The effect of periodic arrays of feedback shunted piezoelectric (PZT) patches in vibration attenuation of flexible beams is analyzed theoretically and experimentally. Each pair of surface-bonded piezoelectric patches is linked with a uniform and isolated feedback circuit. The voltage generated by one piezoelectric patch of the pair is amplified and applied to the other. Numerical model based on the transfer matrix methodology are developed to predict the transmission of vibration and the frequency ranges of band gaps in the proposed periodic smart structure. Broadband vibration attenuations are observed no mater in or out of the band gaps. The proposed concept is validated on a suspended epoxy beam driven by a shaker. Experimental results are presented in terms of vibration transmissions recorded using two accelerometers placed on both sides of the beam.

As illustrated in Fig. 1, pairs of PZT patches are periodically stuck to the surface of a beam to construct a 1D PC. Each pair of PZT patches are placed with opposite polarizing directions along the *z*-axis and linked with a uniform shunting circuit. The beam's segments with the PZT patch are denoted as I, while the others are denoted as II. Each shunting circuit is composed a operational amplifier (opamp) and two resistors R_1 and R_2. The voltage signal from one PZT patch is amplified and adds on the other. We call it the feedback shunts.

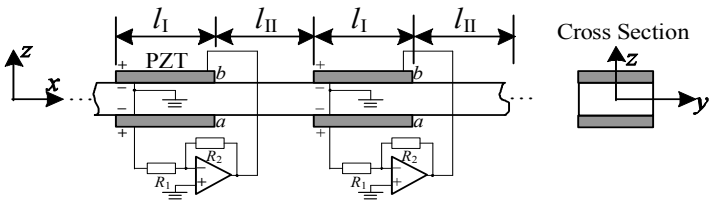

Figure 1 Beam with arrays of PZT patches and feedback shunting circuits.

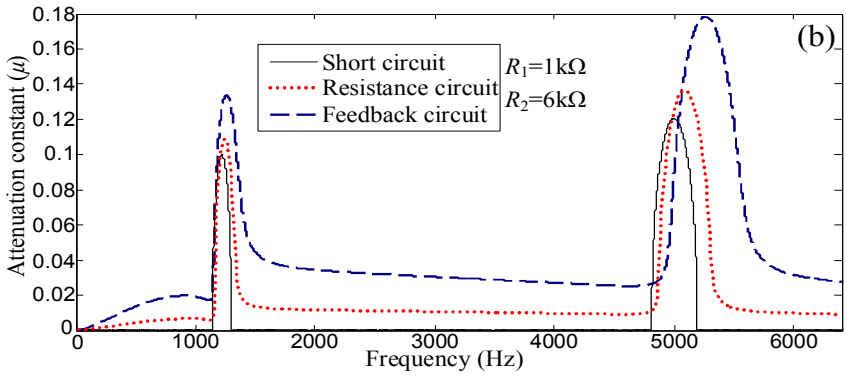

Figure 2 Calculated attenuation constants of the one-dimensional phononic crystals composed of an epoxy beam and shunted PZT patches. The solid, dotted and dashed lines represent the results for short, resistance, and feedback shunting circuits respectively.

Figure 2 illustrates the calculated attenuation constants of 1D PCs containing different shunting circuits. The dashed lines in Fig. 3 represent the results corresponding to the feedback shunting circuit

Phononics 2011: First International Conference on Phononic Crystals, Metamaterials and Optomechanics
Santa Fe, New Mexico, USA, May 29-June 2, 2011
PHONONICS-2011-0067

in this paper. For comparison, results corresponding to the resistance (R_1) shunting circuit and short circuit are also calculated and illustrated as solid and dotted lines in Fig. 2, respectively. Compared with other shunting circuits, the feedback one can evidently increase the attenuations at almost all frequencies no matter in or out of band gaps. In detail, original band gaps are widened and the corresponding attenuations are strengthened. Moreover, the attenuations out of band gaps that caused by damping are also enlarged dramatically by the feedback shunting circuits.

To validate the theoretical results, vibration experiments were performed on a 1D PC composed of an epoxy beam and periodic arrays of PZT-5H patches. The total length of the beam was 0.64 meters, where a periodic structure with 8 periods is constructed.

Figure 3 illustrated the measured transmission of the 1D PC. The overall view of the experimental results is shown in Fig. 3(a), while other subfigures (b)-(d) are zoomed in view of Fig. 3(a) within different frequency ranges. For comparison, the transmission of the 1D PC with short cut circuits, i.e., all electrodes of the PZT patches are shorted, is plotted as thin solid line in Fig. 3. All the experimental results illustrate in Fig. 3 basically match with the theoretical predictions. Moreover, the dashed and dotted lines in Fig. 3 represent the results corresponding to that only 5 or 2 PZT patches near the exciting point that are connected to the feedback shunting circuits. Coinciding with a basic characteristic of PCs, the attenuations are always weakened proportionally when the number of periodicity decreases.

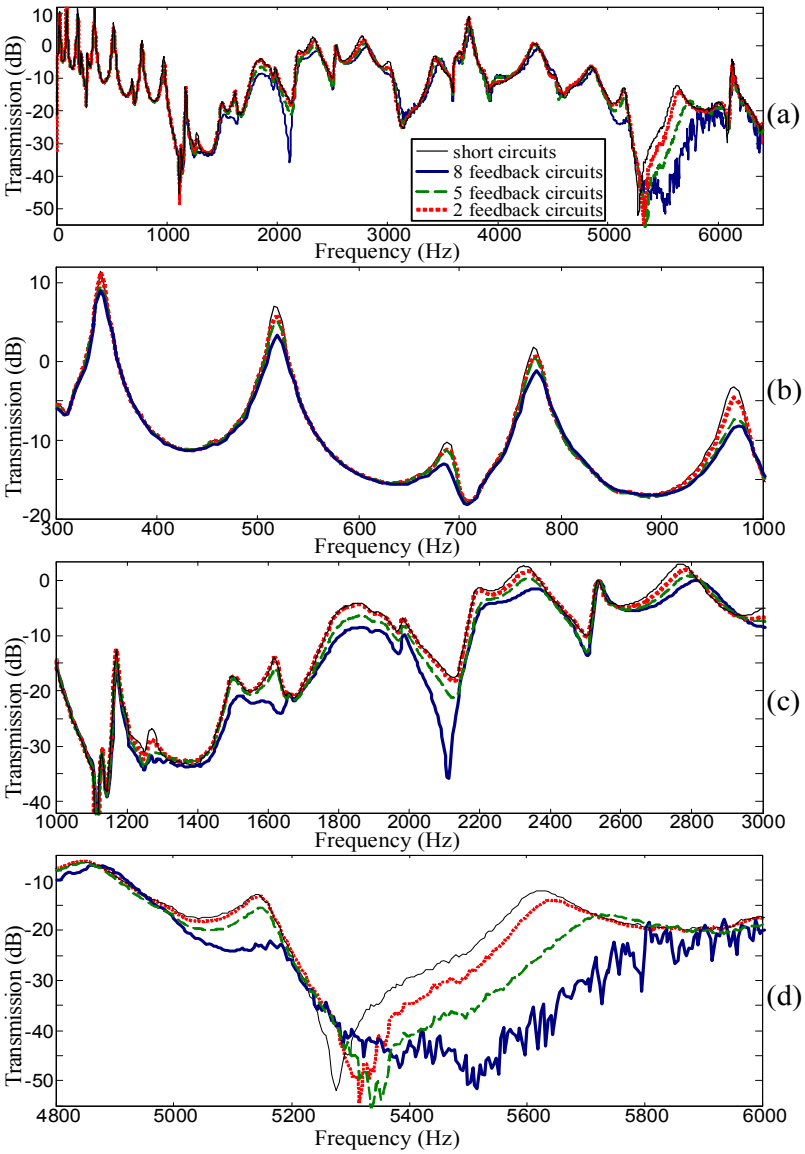

Figure 3 Measured transmission of the 1D phononic crystal with feedback shunting circuits. The thick solid lines, dashed line and dotted line represent the results corresponding to the cases when 8, 5 and 2 PZT patches near the exciting point are connected with the feedback shunting circuits, respectively. The thin solid lines represent the result when all electrodes of the PZT patches are shorted and are used for comparison.

Phononics 2011: First International Conference on Phononic Crystals, Metamaterials and Optomechanics
Santa Fe, New Mexico, USA, May 29-June 2, 2011
PHONONICS-2011-0069

Phase-controlling properties in phononic crystals

N. Swinteck [1], S. Bringuier [1], J.-F. Robillard [2], J.O. Vasseur [2], A.C. Hladky [2] and P.A. Deymier [1]

[1]*Department of Materials Science and Engineering, University of Arizona, Tucson, Az 85721, USA*

[2]*Institut d'Electronique, de Micro-électroniqueet de Nanotechnologie, UMR CNRS 8520, CitéScientifique, 59652 Villeneuve d'AscqCedex, France*

swinteck@email.arizona.edu

Abstract: We deliver a complete phase-space analysis of two well-studied PC systems to reveal the mechanisms behind phase-manipulation of propagating elastic waves in these composite structures. A triangular-array of steel cylinders embedded in a host matrix of methanol and a square-array of Polyvinylchloride cylinders embedded in a host matrix of air show band structures and equi-frequency contours (EFCs) with very different features, yet phase-control is possible in both systems. We find that phase-control depends on (1) whether or not the wave and group velocity vectors in the PC are collinear and (2) whether or not the excited Bloch waves in the PC have the same phase velocity. The results gathered in this study can be used to draw general conclusions about the reality of phase-control in many other types of PCs.

Phononic crystals (PCs) are composite materials comprised of periodic arrays of elastic inclusions embedded in an elastic matrix. The majority of research in the field of phononics has been aimed at understanding how the scattering of elastic waves impacts the spectral and wave-vector properties of the crystal. Past efforts have shown PCs with numerous, useful properties including transmission band gaps, local wave-guiding modes, filtering and multiplexing capabilities, and unique refractive behavior [1-4]. Several functional acoustic devices have resulted from exploitation of these exceptional properties. Progress in the field of phononics is directly coupled to the development of new acoustic based technologies, and for this, it is important for researchers to adventure beyond the contemporary functionalities of today's PCs.

An avenue that has been overlooked in the field of phononics is the impact PCs have on the relative phase of propagating elastic waves. The concept of phase-control between incident waves in any PC can be realized through thorough analysis of its band structure and equifrequency contours (EFCs). One condition must firstly be satisfied for the possibility of phase-control: all incident elastic waves that are transmitted through the PC must have an associated Bloch wave with a non-zero degree of refraction. If the degree of refraction for all incident waves is zero, then the projection of each wave vector in the PC onto the direction consistent with the group velocity vector is the same and a phase-shift cannot possibly result. The EFC corresponding to this very unique scenario is a perfect square either centered on or off the gamma point. With the knowledge that positive or negative refraction must occur, there are two general schemes amongst PC EFCs that outline the possibility for phase-control. One scheme is where the phase velocity of all excited Bloch modes is identical—a circular EFC centered on the Gamma point has such a property because the magnitude of all wave vectors in the PC is the same. A relative phase-shift between propagating waves in this type of PC comes from waves of the same phase velocity traveling different distances through the crystal. The second scheme applies to most PC EFC structures. In the case where wave vectors in the PC are non-collinear with group velocity vectors (phase velocities of Bloch waves are different) and each excited Bloch wave has a unique degree of refraction, a relative phase shift occurs

Phononics 2011: First International Conference on Phononic Crystals, Metamaterials and Optomechanics
Santa Fe, New Mexico, USA, May 29-June 2, 2011
PHONONICS-2011-0069

between propagating waves. Each wave vector in the PC projects differently onto its associated path of propagation (group velocity vector) and the phase velocity of the excited mode is different along this path, giving a slightly different quantification for phase shift as compared to scheme one. Interestingly, since these two scenarios apply to most types of PC EFCs, phase-control can be realized with a large number of different PCs. Changing the incident angles of the elastic waves entering the PC, varying the PC length, and altering the initial relative phase between input signals, are some means of controlling the output signal of the PC device. Such knowledge can possibly enhance the performance of current acoustic based technologies utilizing PCs and lead to completely novel concepts of future phononic devices.

We investigate the phase-properties of two PCs to link EFC features with the phase-relationship between propagating elastic waves. Our first PC is a triangular lattice of steel cylinders embedded in a host matrix of methanol, all in water. The diameter of the inclusions is 1.02 mm and the lattice spacing is 1.27 mm. Our second PC is a square lattice of Polyvinylchloride (PVC) cylinders embedded in a host matrix of air, all in a surrounding environment of air. The diameter of the inclusions is 25.8 mm and the lattice spacing is 27 mm. The first PC, at an operating frequency of 530 – 570 kHz, has a circular EFC centered on the Gamma point whereby the wave and group velocity vector are collinear and the phase-velocity of all excited Bloch modes is identical. The second PC, at an operating frequency of 13.5 kHz, has a square-like EFC centered off the Gamma point. Here, the wave and group velocity vectors are non-collinear and each excited Bloch mode has a unique phase velocity associated with it. Figure 1 shows the relative phase-shift between several pairs of incident acoustic waves for the PC consisting of a triangular lattice of steel cylinders embedded in a host matrix of methanol (550 kHz). Figure 2 shows the relative phase-shift between several pairs of incident acoustic waves for the PC consisting of a square lattice of PVC cylinders embedded in a host matrix of air (13.5 kHz). By utilizing the phase-information contained in Figure 2 and including an additional assessment for the phase-shift incurred on the exit side of the PVC-Air PC, we demonstrate complete control over the relative phase of two acoustic inputs by modulating their initial relative phase by π and 2π radians. Figures 3a and 3c show finite-difference-time-domain simulations (plots of instantaneous pressure) of two acoustic beams entering the PVC-Air PC. Figure 3a shows a crystal of length 621mm and Figure 3c shows a crystal of length 1242 mm. The time average of instantaneous pressure taken over one cycle (reported as average pressure) is shown in Figures 3b and 3d. Average pressure readings are taken along cuts where the acoustic beams intersect (black lines in Figures 3a and 3c). If the beams are in-phase, the average pressure reading will yield a maximum. If the beams are out of phase, the average pressure cut will show a minimum. Figure 3b shows that with a crystal of length 621mm, we observe a change in relative phase of π—the input average pressure cut shows a minimum, while the output average pressure cut shows a maximum. Figure 3d shows that with a crystal of length 1242mm, we observe a change in relative phase of 2π— the input average pressure cut shows a minimum and the output average pressure cut shows a minimum. This demonstrates a phase modulation of π and 2π radians based solely on changing the PC length. Similar control can be achieved by altering the angles and keeping the PC length constant. This is one example, of many, where precise phase-control exists between acoustic beam pairs.

Phononics 2011: First International Conference on Phononic Crystals, Metamaterials and Optomechanics
Santa Fe, New Mexico, USA, May 29-June 2, 2011
PHONONICS-2011-0071

New Directions in the Analysis of Nano-Scale Phononic and Nonlinear Metamaterial Systems

Michael J. Leamy[1]

[1] *George W. Woodruff School of Mechanical Engineering, Georgia Institute of Technology,771 Ferst Drive N.W., Atlanta, GA, USA*
michael.leamy@me.gatech.edu

Abstract: This talk will focus on two directions being pursued by the author and his co-workers in the areas of (i) multi-scale modeling of phonon spectra and dispersion in reduced dimensional nano-scale systems (e.g., carbon nanotubes), and (ii) analysis of phononic wave propagation in nonlinear metamaterials using asymptotic techniques.

The first part of this talk will address a multi-scale modelling approach being pursued by the author for predicting phonon spectra and dispersion in reduced dimensional materials, such as graphene sheets, nanotubes, and nanotoroids. For reduced-dimension nanophononic systems with large unit cells (e.g., 'supercells' housing defects or unit cells capturing non-ideal geometries such as embodied by 'wavy' nanotubes), manifold-based finite element modelling is advantageous for several reasons, to include large reduction in degrees of freedom, applicability to complex geometries, and the presence of a natural curvilinear basis for describing wave vector components. Reduced-dimension materials are quite unlike full-dimensional materials in that they are neither space-filling nor simply-connected, and thus require manifolds for representation. For example, a carbon nanotube unit cell must fully wrap around the circumference in order to truly repeat, which results in two ends of the unit cell sharing the same atoms. This complex geometry can be described efficiently using an intrinsic set of basis vectors whose (reduced) dimension equals the dimension of the manifolds describing the system. Continuum modeling on manifolds generates the necessary basis vectors, while significantly reducing the degrees of freedom.

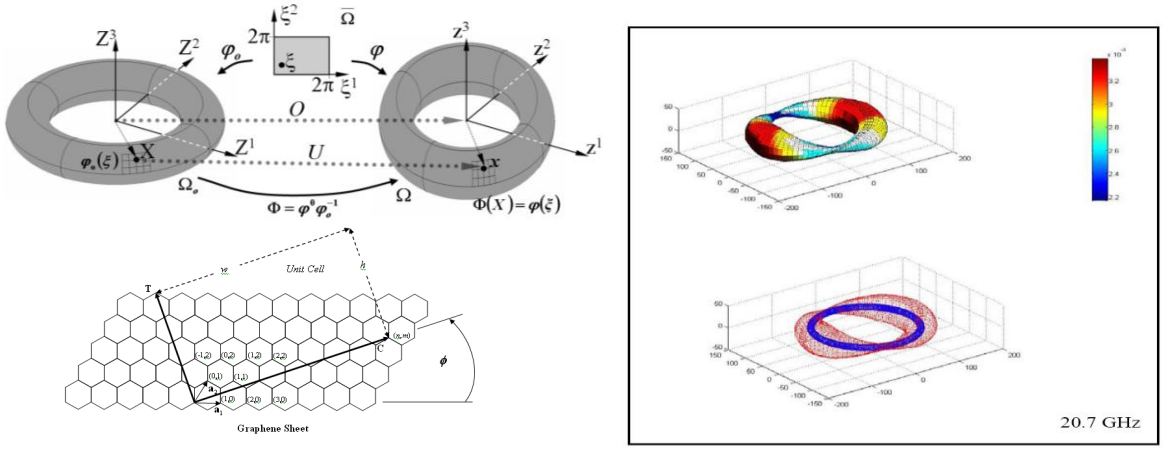

Figure 1 (a) Continuum computation approach used to study reduced-dimension materials. Intrinsic basis vectors $\boldsymbol{G}^i$ and the use of representative area elements to sample interatomic potential energy allow the phonon spectra to be accurately predicted. **(b)** Typical acoustic mode of vibration predicted using the continuum approach.

A recently-developed multi-scale continuum approach[1] forms the basis for reduced-order modeling of the reduced-dimension nanophononic systems (see Fig. 1a for an example nanotoroid) discussed during the talk. This approach employs intrinsic basis vectors defined on a reduced-dimension surface (manifold) of the nanostructured material. Changes in interatomic potential energy arising from lattice vibrations are equated to changes in continuum strain energy, allowing non-quantum atomistic beha-

Phononics 2011: First International Conference on Phononic Crystals, Metamaterials and Optomechanics
Santa Fe, New Mexico, USA, May 29-June 2, 2011
PHONONICS-2011-0071

vior to be captured using continuum techniques. The energy change is sampled using representative area elements. A subsequent finite element discretization results in a significant decrease in the deformation degrees of freedom present, while at the same time accurately capturing the acoustic range of the phonon spectra. Figure 1b displays a typical acoustic mode of vibration predicted using this procedure. Applying Bloch analysis, dispersion relationships have also been obtained and will be discussed during the talk. In particular, the author will discuss the accuracy of the obtained acoustic and optic branches, and will discuss in general what can be expected from any multi-scale approach.

The second part of this talk will address asymptotic techniques being developed by the author and his co-workers for analyzing wave propagation in nonlinear periodic metamaterials. Gigahertz communication devices, such as mobile phones, use phononic-based systems for their low-power filtering characteristics. Many sensing devices based on resonators, acoustic logic ports, and surface acoustic wave-based filters rely on the unique band gap characteristics of phononic crystals, an important class of periodic metamaterials. The majority of recent research on wave propagation in periodic metamaterials has been devoted to linear media, with little attention paid to characterize, analyze and exploit the effects of nonlinearities for wave propagation management and control. As devices miniaturize further, nonlinear behavior becomes the norm and not the exception, as witnessed in part by the complex potentials used to describe small-scale interactions. The effects nonlinearities exert on dispersion characteristics, band-gaps, and directionality have not been the focus of a concerted research effort, and as a result are not well-understood. Most importantly, nonlinearities should be explored as means to achieve novel functionalities which potentially enrich the design space of periodic media.

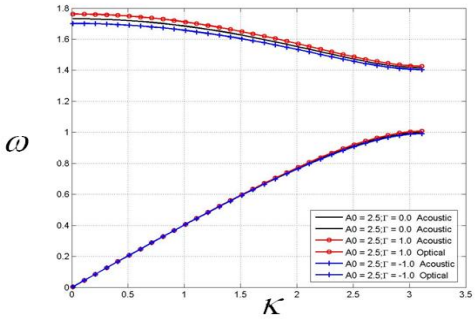

Figure 2 Amplitude-dependence of diatomic chain's dispersion behavior.

The considerations above have led us to investigate discrete (and continuous systems following discretization) of the following form,

$$\mathrm{M}\ddot{\underline{u}}_j + \mathrm{K}\underline{u}_j + \underline{F}^L(u_{j-1,N}, u_{j+1,1}) + \varepsilon \underline{F}^{NL}(\underline{u}_j, u_{j-1,N}, u_{j+1,1}) = 0\,, \tag{1}$$

where the displacement vector $\underline{u}_j = [u_{j,1}\ u_{j,2}\ u_{j,3}\ldots..\ u_{j,N}]^T$ contains the displacements of the masses of the j^{th} unit cell, the unit cell mass and stiffness matrices are denoted by $\mathrm{M} \in R^{N\times N}$ and $K \in R^{N\times N}$, and $\underline{F}^L \in R^{N\times 1}$ contains linear restoring forces associated with masses *neighboring* the unit cell while $\underline{F}^{NL} \in R^{N\times 1}$ contains all nonlinear restoring forces. As such, (1) governs an open set of nonlinear difference equations and therefore requires a solution procedure unlike that traditionally used in weakly nonlinear systems. However, ideas similar in spirit to the Lindstedt-Poincaré and multiple scales perturbation techniques have been developed by the author and co-workers to solve for amplitude-dependent dispersion relations corrected up to second order[2,3].

Figure 2 plots the dispersion trend for the two wave modes predicted by the perturbation analysis of a cubically-hardening chain. The trends pictured have been verified via comparison with numerically simulated diatomic chains[2]. The figure demonstrates that an increase in wave amplitude shifts both dispersion branches upwards, effectively moving (or tuning) the band gap location. We have also predicted similar dispersion shifts when multiple waves interact[3]. Possible devices exploiting this amplitude-dependent dispersion behavior will be discussed during the talk.

References

[1] Leamy, M.J., and DiCarlo, A., *Comput. Method. Appl. M.* **198**, 1572-1584 (2009).
[2] Narisetti, R.K., Leamy, M.J., and Ruzzene, M., *J. Vib. Acoust.* **132**(3): 031001 (2010).
[3] Manktelow, K., Leamy, M.J., and Ruzzene, M., 2010, *Nonlinear Dyn.* **63**, 193-203.

Phononics 2011: First International Conference on Phononic Crystals, Metamaterials and Optomechanics
Santa Fe, New Mexico, USA, May 29-June 2, 2011
PHONONICS-2011-0076

An Effective Medium Model for Sonic Crystals with Composite Resonant Elements

Olga Umnova[1] , Anton Krynkin[1], Alvin Y.B.Chong[2], Shahram Taherzadeh[2], Keith Attenborough[2]

[1] Acoustics Research Centre, The University of Salford, Salford, Greater Manchester, UK, o.umnova@salford.ac.uk, a.krynkin@salford.ac.uk
[2] Department of Design Development, Environment and Materials, The Open University, Milton Keynes, UK y.b.a.chong@open.ac.uk, s.taherzadeh@open.ac.uk, k.attenborough@open.ac.uk

Abstract: Using a self-consistent method, analytical expressions are derived for the parameters of an effective medium of composite scattering elements in air. The scatterers consist of concentrically arranged thin elastic shells and 4-slit cylinders. Predictions and data confirm that the use of coupled resonators results in a substantial insertion loss peak related to the modified resonance of the shell.

Periodic arrays of resonant scatterers such as thin elastic shells [1] or split ring resonators [2-3]can support low frequency band gaps in addition to those associated with array periodicity [1]. With finite periodic arrays they correspond to frequency intervals of low transmission and lead to an improved attenuation below the first of the Bragg's band gaps. To describe low frequency behaviour, an effective medium model has been developed for an array of c concentrically arranged hollow rigid cylinderswith multiple slits (N-slit rigid cylinder) and thin elastic shells (Fig.1).

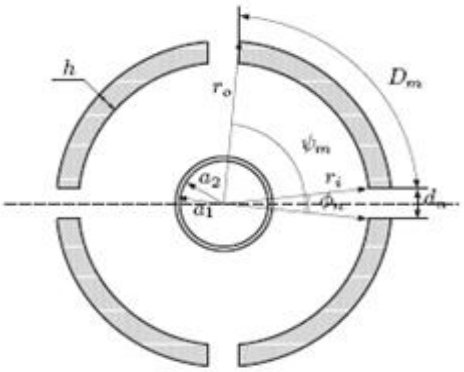

Figure 1. Cross-section of composite element consisting of a concentric arrangement of an outer 4-slit rigid cylinder and an inner elastic cylindrical shell.

The composite scatterer is a system of coupled resonators and gives rise to multiple resonances. The corresponding analytical model employs polar angle dependent boundary conditions on the surface of N-slit cylinder. The solution inside the slits assumes plane waves. The simplified low frequency description of the composite scatterer relies on the replacement of the N-slit cylinder by an equivalent fluid layer. The concentric arrangement results in resonances associated with both circular and annular cavities. An axisymmetric resonance of the shell is preserved but shifted to the lower frequency range by the presence of the cavity. This is similar to the effect observed in mass-spring system with multiple degrees of freedom.

Using a self-consistent approach [4], e analytical expressions are derived for the characteristic impedance and the wavenumber of an effective medium comprised of composite scatterers in air. The approximation is applicable when wavelengths in both air and effective medium exceed the size of a single scatterer. The model takes into account viscoelastic losses in the shells. The effective medium model predictions are compared with the solutions for infinite doubly periodic arrays and insertion loss data for finite arrays of composite scatterers. In laboratory experiments 2m long and 0.25mm thick Latex cylinders with outer diameter of 43mm and 55mm outer diameter slitted PVC pipes were used. Concentric arrangements of pairs of Latex and 4-slit PVC cylinders were formed as shown in Figure 1.The cylinders were arranged in a periodic (square) array with lattice constant of 8cm. The Bragg frequency for the array is around 2kHz. It is demonstrated that the model predicts negative real part of the effective compressibility around the modified axisymmetric shell resonance (Fig.2) at 1.1kHz.

Phononics 2011: First International Conference on Phononic Crystals, Metamaterials and Optomechanics
Santa Fe, New Mexico, USA, May 29-June 2, 2011
PHONONICS-2011-0076

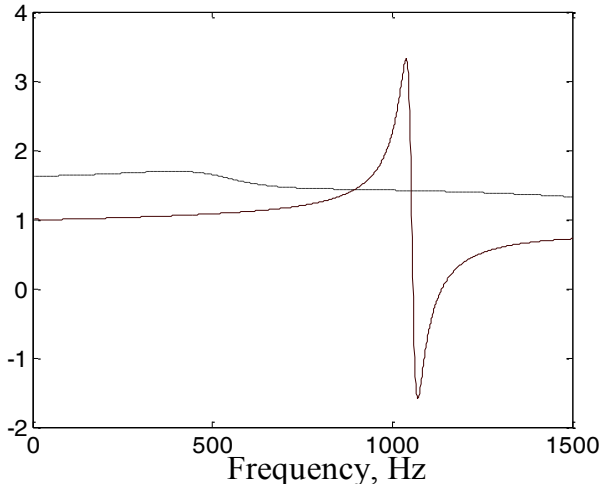

Figure 2. Real part of normalised effective density (– –) and effective compressibility (——) as a function of frequency.

As shown in Fig. 3, for an array of 21 composite scatterers the effective medium model correctly predicts the frequency of the corresponding insertion loss peak, but overestimates its value.

Plane waves were assumed and the array was modelled as infinitely wide slab. One of the reasons for disagreement is the limited validity of the plane wave approximation; the second is the inapplicability of the long wave approximation around the resonant frequency. A better agreement is obtained between the effective medium model and multiple scattering theory predictions for larger arrays with receiver placed further away from the array. Characteristic impedance and wavenumber are deduced from laboratory data and predictions of the multiple scattering theory using methods developed in paper [5] and compared with those predicted by the effective medium model.

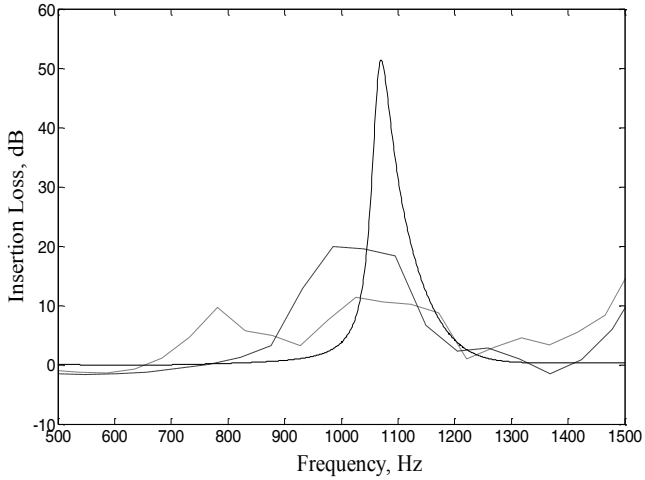

Figure 3. Multiple scattering (– –) and effective medium (——) predictions compared with data (– - –) for 7X3 array of composite scatterers. Distances to the source and receiver are 1.5m and 0.05m, respectively.

References

[1] A.Krynkin, O.Umnova, A.Y.B.Chong, S.Taherzadeh and K.Attenborough,, *J.Acoust.Soc.Am*, **128,** 3496-3506 (2010).
[2] A.B.Movchan, S.Guenneau, *Phys.Rev.B*, **70**, 125116 (2004)
[3] S.G.L.Smith, A.M.J.Davis, *Proc.R.Soc.A*, **466**, 3117-3134 (2010)
[4] J.G Berryman, *J.Acoust.Soc.Am*, **68,** 1809-1819 (1980).
[5] V.Fokin, M.Ambati, C.Sun, X.Zhang, *Phys.Rev.B* **76**, 144302 (2007)

Phononics 2011: First International Conference on Phononic Crystals, Metamaterials and Optomechanics
Santa Fe, New Mexico, USA, May 29-June 2, 2011
PHONONICS-2011-0079

Control of Vibrational Energy in Nonlinear Granular Crystals

Georgios Theocharis[1], **Nicholas Boechler**[1], **Chiara Daraio**[1]

[1] *Graduate Aerospace Laboratories (GALCIT) California Institute of Technology, Pasadena, CA 91125, USA*
georgiostheocharis@gmail.com boechler@caltech.edu daraio@gmail.com

Abstract: We describe recent work on nonlinear granular crystals. We explore phenomena related to vibrational energy localization, re-distribution, and rectification enabled by the spatial discreteness, disorder, and nonlinearity of granular crystals. In addition, we note how an understanding of dynamic phenomena in granular crystals can enable the design of novel engineering devices.

The ability of periodic structures to affect wave propagation – through the existence of phenomena such as band gaps – has been studied across a wide array of fields. This includes the propagation of light in photonic crystals and elastic/acoustic waves in phononic crystals[1]. The scalability of such concepts has been shown, at the intersection of these two fields, in the development of optomechanical crystals[2], which produce phononic waves as a result of photonic excitation. However, the majority of these studies have focused on the linear dynamical behaviour of these systems. Although studying the linear response is an important first step, it is more often the exception than the rule in naturally occurring systems. Nonlinear systems, albeit more difficult to study, are more general, and offer the possibility of new phenomena and functionality.

Granular crystals are systems composed of a tightly packed array of elastically interacting particles. With the Hertzian contact that governs the interaction between the particles, granular crystals are both spatially discrete (dispersive) and nonlinear systems. Granular crystals have drawn recent interest due to the tunability of their dynamic vibrational response (with the application of a static load) to encompass linear, weakly nonlinear, and strongly nonlinear regimes; the simplicity of their construction; and their applicability to engineering devices[3]. The study of granular crystals has seen the emergence of coherent structures such as solitary waves[3], intrinsic and extrinsic nonlinear localized modes[4,5], and other nonlinear phenomena such as tunable frequency band gaps[4], bifurcations[6], and chaos[7].

Here we show a specific example of a nonlinear coherent structure, a discrete breather (DB), which can be found in granular crystals. DBs have been a central theme for numerous theoretical studies while the past several years they have been observed in a myriad of physical systems ranging from biological to microengineered and condensed matter systems covering all the length scales [8]. In Fig. 1, we show an experimental observation of a DB, generated in an 80 particle diatomic granular crystal. This example shows how the interplay of nonlinearity and discreteness/periodicity leads to the localization of vibrational energy to a narrow spatial regime, at a specific frequency. The underlying physical mechanism, as described in[4], that leads to the development of an intrinsically localized mode, is the modulational instability of the lower optical cutoff mode of the diatomic granular crystal. A systematic study of the existence and stability of these nonlinear localized vibrations in a diatomic granular crystal can be found in[5].

In contrast with traditional types of localization in disordered media, the discrete breathers are "intrinsic" as they do not require the presence of any defects, and can occur in perfectly periodic chains. However, the inclusion of an extrinsic disorder in granular crystals, in combination with their nonlinear response, leads to other interesting phenomena such as nonlinear defect modes and symmetry breaking bifurations[6]. Such modes allow the response of the system to be tunable, not only with the application of static load, but with a change in the amplitude of the propagating wave; another example of increased functionality resulting from nonlinearity. Furthermore, in the presence of a defect and a driver at one end of the chain, hopf bifurcations can lead to the appearance of quasiperiodic and chaotic vibrations in granular crystal systems[7]. Such instabilities and bifurcations, resulting from, and in combination with nonlinearity, enables the re-distribution of energy amongst other frequencies of

Phononics 2011: First International Conference on Phononic Crystals, Metamaterials and Optomechanics
Santa Fe, New Mexico, USA, May 29-June 2, 2011
PHONONICS-2011-0079

the system – a characteristic previously unavailable to linear systems. Taking advantage of such phenomena, we have proposed a tunable rectifier of vibrational energy[7]. Such a system could have importance in a wide array of applications, including: biomedical imaging technologies, vibrational and thermal energy logic systems, and energy harvesting devices.

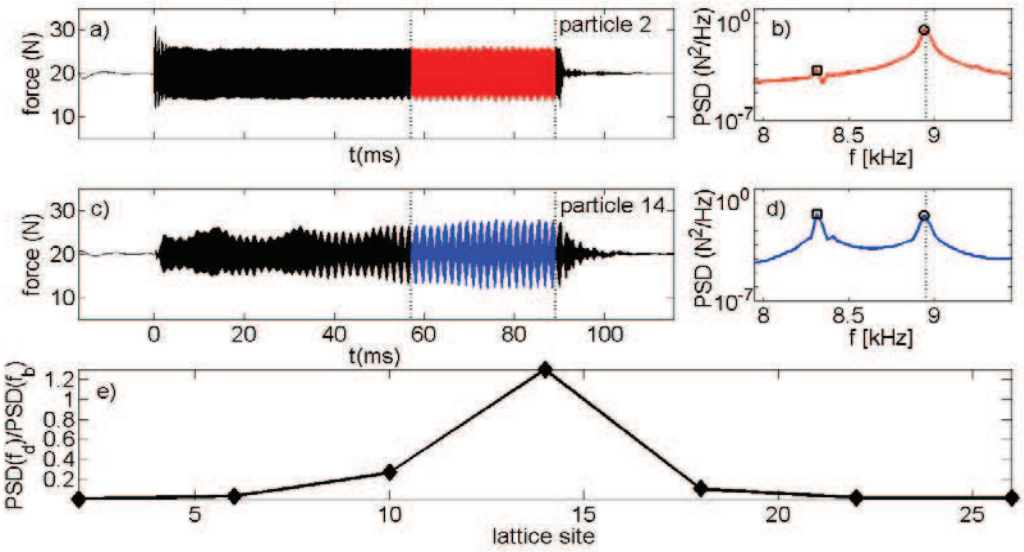

Figure 1: Experimental observation of a DB, in an 80 particle granular crystal, at f_b=8.31 kHz. **(a),(b)** Force at particle 2 and 14, respectively. **(c),(d)** Power spectral density (PSD) for the highlighted time regions in **(a),(c)** of the same color. Square [circular] markers denote the DB [driving] frequency and PSD amplitude. **(e)** The ratio of the PSD amplitude at the discrete breather frequency divided by the PSD amplitude of the driving frequency as a function of sensor location. The vertical dashed line in **(b)** and **(d)** denotes the lower cutoff frequency of the optical band, and the vertical dashed lines in **(a)** and **(c)** denote the time region for the PSD calculation.

Mirroring the evolution of the study of photonic crystals, we aim to extend the study of the emerging field of phononics into the realm of nonlinearity. Nonlinearity has the potential to break the restrictions imposed by linearity, and enable the design of new devices. This includes mechanisms for controlling the spatial distribution of vibrational energy, and for the conversion of energy to other frequency waveforms. In granular crystals, we have found a useful test-bed and model for such an investigation. Accordingly, we have also developed the theoretical, numerical, and experimental tools for furthering the understanding of nonlinear phononic phenomena, and developing novel applications.

References

[1] T. Gorshnvyy, M. Maldovan, C. Ullal, E. Thomas, *Phys. World*, **18**, 24 (2005).
[2] M. Eichenfield, J. Chan, R. Camacho, K. J. Vahala, O. Painter, *Nature*, **462**, 78 (2009).
[3] V. F. Nesterenko, *Dynamics of Heterogeneous Materials,* Springer-Verlag, New York, USA (2001).
[4] N. Boechler, G. Theocharis, S. Job, P. G. Kevrekidis, M. A. Porter, and C. Daraio, *Phys. Rev. Lett.* **104**, 244302 (2010).
[5] G. Theocharis, N. Boechler, P. G. Kevrekidis, S. Job, M. A. Porter, and C. Daraio, *Phys. Rev. E* **82**, 056604 (2010).
[6] G. Theocharis, G.; Kavousanakis, M.; Kevrekidis, P. G.; Daraio, C.; Porter, M. A. and Kevrekidis, Y., *Phys. Rev. E* **80**, 066601 (2009).
[7] N. Boechler, G. Theocharis, and C. Daraio, *in preparation* (2011).
[8] S. Flach and A. V. Gorbach, *Phys. Rep.* **467**, 1 (2008).

Phononics 2011: First International Conference on Phononic Crystals, Metamaterials and Optomechanics
Santa Fe, New Mexico, USA, May 29-June 2, 2011
PHONONICS-2011-0098

Second harmonics, instabilities and hole solitons in 1D phononic granular chains

Víctor J. Sánchez-Morcillo[1*], I. Pérez-Arjona[1], V. Gusev[2], V. Tournat[3]

[1] IGIC, Universidad Politécnica de Valencia, Paranimf 1, 46730 Grau de Gandia, Spain,
[2] LPEC, [3] LAUM, CNRS, Université du Maine, Av. Olivier Messiaen 72085, Le Mans, France
**victorsm@upv.es*

Abstract: The propagation of nonlinear compressional waves in a 1D compressed granular chain driven at one end by a harmonic excitation is theoretically studied. The chain is described by a FPU lattice model with quadratic nonlinearity. We predict and describe different nonlinear phenomena, as the generation of second harmonics, modulational instabilities and the existence of hole (or dark) solitons.

We consider the propagation of a harmonic signal applied to one end of a homogeneous 1D chain of spherical beads in contact, each with a mass *m* and a radius *R*, as shown in Fig. 1. Under the effect of an external constant force F_0 [Fig.1] the chain is compressed, and the distance between centers is reduced by an amount δ_0 resulting in $a = 2R-\delta_0$. Denoting by u_n the displacement of the *n*-th bead from its equilibrium position, and assuming that the beads repel upon Hertz-type potential $V(\delta) \propto \delta^{5/2}$, with $\delta = \delta_0 - (u_n - u_{n-1})$ being the bead-bead overlap, the dynamics of the chain is described by a system of coupled ordinary differential equations for the displacements, which for $\delta_0 >> | u_n - u_{n-1} |$ can be written as a quadratic FPU equation, as [1]

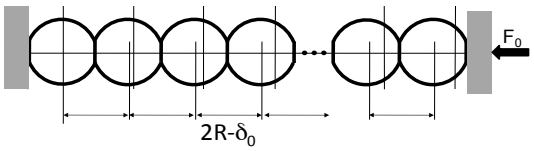

Figure 1 1D chain of spherical beads in contact compressed by an external constant force.

$$\frac{\mathrm{d}^2 u_n}{\mathrm{d}t^2} = \frac{1}{4}\left(u_{n+1} - 2u_n + u_{n-1}\right) - \frac{\varepsilon}{8}\left(u_{n+1} - 2u_n + u_{n-1}\right)\left(u_{n+1} - u_{n-1}\right) \qquad (1)$$

where $\varepsilon = u_0 / 2\delta_0$ is the nonlinearity parameter. We consider a driven lattice, subjected to the boundary condition $u_0(t) = \sin(\Omega t)$, being Ω the driving frequency. Neglecting nonlinearity, we obtain the dispersion relation of the chain, $\Omega = \left|\sin\left(k/2\right)\right|$ defining the cutoff frequency Ω=1.

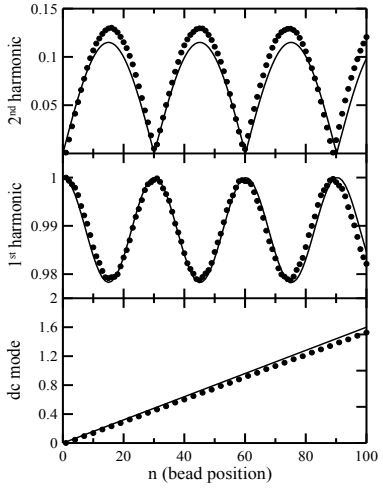

A successive approximations method is used to find the analytical expressions for the amplitudes of the static displacement field, and of the fundamental and second harmonics propagating through the lattice. We distinguish two regimes, depending on whether the second harmonic is a propagating (0<Ω<1/2) or evanescent (1/2<Ω<1) mode. The results for the propagative case are shown in Fig. 2, where we depict the amplitude of the different modes. Note the mode beating induced by the lattice dispersion. In both cases, it is found that second harmonic is present, and influences the propagation characteristics of the fundamental mode. The comparison of the analytical results (full lines) and numerical results (dots) is shown in Fig. 2.

Figure 2. Amplitudes of the different modes (static, fundamental and second harmonic) in the case ε=0.1 and Ω=0.4 (propagative case) along the chain, for the first 100 beads. Note the linear growth of the static mode, and the beatings of fundamental and second harmonics.

Phononics 2011: First International Conference on Phononic Crystals, Metamaterials and Optomechanics
Santa Fe, New Mexico, USA, May 29-June 2, 2011
PHONONICS-2011-0098

The successive approximations method allows predicting the amplitudes of the different modes propagating in the chain, but is not appropriate to study other dynamical effects induced by the nonlinearity, like instabilities or envelope solitons. In other to study these phenomena, a technique based in a multiple scales expansion method together with the so-called quasi-discreteness approximation [2] is used instead. Considering both slow temporal and spatial scales, the following equation for the envelope A of the fundamental wave can be obtained:

$$\frac{\partial A}{\partial \tau} = iP\frac{\partial^2 A}{\partial x_n^2} + iQ|A|^2 A, \tag{2}$$

where $P = \frac{1}{2}\frac{\partial^2 \Omega}{\partial k^2}$ is the dispersion coefficient, $Q = \frac{1}{4}\Omega\left(1-3\Omega^2\right)\varepsilon^2$ the nonlinearity coefficient and we have defined the retarded time $\tau = t - x_n / v_g$ where x_n identifies the bead position and v_g the group velocity. Equation (2) is the well-known Nonlinear Schrödinger (NLS) equation. The NLS equation provides a canonical description for the envelope dynamics of a quasi-monochromatic plane wave (the carrying wave) propagating in a weakly nonlinear dispersive medium when dissipative processes are negligible [3]. From Eq. (2) it follows that the uniform solution is always modulationally unstable when $PQ > 0$, provided some threshold amplitude is reached. This is known as the Benjamin-Feir instability and results in a long-wavelength modulation of the propagating signal, which eventually breaks into a sequence of pulses or bright solitons. Since in Eq. (2) P is always positive, the analysis predicts that constant amplitude solutions (plane waves) can be unstable when $\Omega < \Omega_{mi} = 1/\sqrt{3} \approx 0.577$. On the contrary, when $\Omega > \Omega_{mi}$ and solutions are stable, the chain supports propagative localized solutions known as dark (or grey) hole solitons. They have the analytical expression

$$A = A_0\sqrt{1 - d^2 \sec h^2\left(\frac{x - vt}{L}\right)}e^{i\Theta} \tag{3}$$

which is an exact solution of Eq. (2). The existence and stability of such solutions has been demonstrated numerically, and the results are shown in Fig. 3 for ε=0.3 and Ω=0.8. The temporal behaviour of bead labelled as N=50 is shown at the right. The left picture compares the numerical solution with the analytical profile given by Eq. (3), shown in continuous line. The agreement is excellent, demonstrating the existence of the predicted hole solitons. While bright solitons in granular chains have been deeply studied, this is the first prediction of hole solitons in such discrete systems.

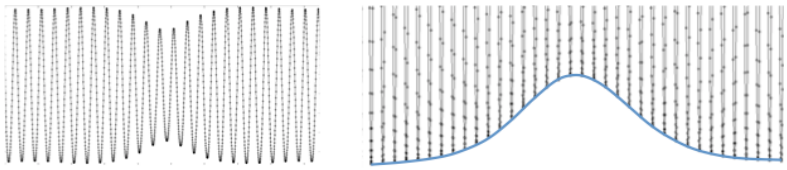

Figure 3. Hole soliton obtained for the case ε=0.3 and Ω=0.8. The temporal behaviour of bead labelled as N=50 is shown.

The work was financially supported by the MICINN of the Spanish Government, under FIS2008-06024-C03-03, and by ANR projects “grANuLar”, NT05-3_41989, and “Stabingram”.

References

[1] V. Tournat, V.E. Gusev and B. Castagnède, Phy. Rev. E 70, 056603 (2004).
[2] T. Taniuti and N. Nayima, J. Math. Phys. 10, 1369 (1969)
[3] C. Sulem and P.L. Sulem, *The Nonlinear Schroedinger Equation*, Springer-Verlag, New York (1999).

Phononics 2011: First International Conference on Phononic Crystals, Metamaterials and Optomechanics
Santa Fe, New Mexico, USA, May 29-June 2, 2011
PHONONICS-2011-0101

Theoretical and Experimental Evidence of Evanescent Modes in Finite Sonic Crystals

V. Romero-García[1,3], L.M. Garcia-Raffi[2], J.V. Sánchez-Pérez[3]

[1] *Instituto de Ciencia de Materiales de Madrid, Consejo Superior de Investigaciones Científicas, Spain*
virogar1@gmail.com,
[2] *Instituto Universitario de Matemática Pura y Aplicada, Universidad Politécnica de Valencia, Spain*
lmgarcia@mat.upv.es
[3] *Centro de Tecnologías Físicas: A.M.A, Universidad Politécnica de Valencia, Spain,*
virogar1@gmail.com, jusanc@fis.upv.es

Abstract: Evanescent modes in complete sonic crystals (SC) and SC with point defects are both theoretically and experimentally reported in this paper. Finite element method and an extension of the plane wave expansion with supercell approximation to solve the invers problem $k(\omega)$ is used to predict the evanescent modes. Experimental data and numerical results are in good agreement with the predictions.

Propagating waves inside a periodic medium represent a set of solutions to the wave equation that satisfy the translational symmetry and they are characterized by the transmission bands obtained using the Bloch's theorem and Fourier expansion of the periodic physical properties. Then the acoustic wave equation can be transformed in an eigenvalue problem and solved using for example the plane wave expanssion (PWE) method. The eigenfrequencies $\omega(k)$ for each Bloch's vector k, inside the irreducible part of the first Brillouin zone constitute the bands structure. One of the most important properties revealed by these bands is the so-called band gaps (BGs): frequency ranges where waves do not propagate through the periodic system. The existence of these BGs leads to the emergence of several interesting physical properties, such as the localized modes within the BG when a point defect is introduced in the structure.

When the translational symmetry is broken, evanescent modes characterized by a complex wave number k, can emerge in these systems. In contrast to infinite periodic media, in the case of the finite ones, the modes inside the BG present evanescent behaviour, growing the decay rate of the mode as the frequency reaches the center of the BG. In Figure 1 we can analyze the evanescent behaviour of a mode inside the BG of a finite Sonic Crystal (SC) made of rigid cylinders with radius $r=0.1$ *m* arranged in square periodicity $a=0.22$ m, at the frequency *920* Hz. The absolute value of the pressure in the points between two rows of the SC has been numerically calculated, using finite elements method (FEM). The numerical predictions and experimental results are plotted in Figure 1 with black continuous line and connected open red circles respectively. It is possible to observe the decay of the mode with the distance all along the SC. With these experimental results, the decay of the evanescent mode inside the BG can be fitted. In order to fit an exponential decay ae^{bx} the points with maximum values have been chosen. The values of the parameters in the fit are $a=0.05597\pm0.0103$ Pa, and $b=Im(k)=-5.60\pm1.45$ m^{-1}, and

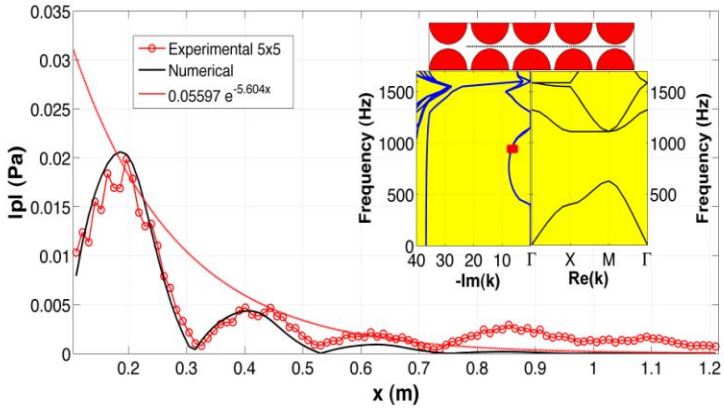

Figure 1 Acoustic pressure inside a 5x5 SC with square array with lattice constant a=22 cm for a frequency inside the BG of 920 Hz. Black continuous line (connected red open circles) represents the absolute values of the numerical (experimental) pressure inside the SC between two rows of scatterers. Red dashed line represents the fitting of the exponential like decay of the measured acoustic field inside the SC. The inset represents the measurement points inside the SC and both the complex and real band structures.

Phononics 2011: First International Conference on Phononic Crystals, Metamaterials and Optomechanics
Santa Fe, New Mexico, USA, May 29-June 2, 2011
PHONONICS-2011-0101

the result is plotted in Figure 1 in red dashed line. In the inset of Figure 1, we show the complex band structure calculated using the extended plane wave expansion (EPWE) in order to solve the inverse problem $k(\omega)$ being k possibly complex. The value of the imaginary part of the first harmonic of the wave vector is marked in the complex band structure with a red square. One can see that $Im(k)=-5.6$ m^{-1} at frequency 920 Hz in a complete SC.

One particularly interesting aspect of SC is the possibility to create point defects that confine acoustic waves in localized modes. Because of the locally breaking periodicity of the structure, defect modes can be created within the BG. These defect modes are strongly localized around the point defect[3]: once the wave is inside the defect, it is trapped because the borders of the defect act as perfect mirrors for waves with frequencies in the BG. To analyze the propagation of waves inside periodic structures with defects, authors have traditionally used PWE with supercell approximation. In this work, we develop the supercell approximation to the EPWE. This methodology enables us to obtain the relation $k(\omega)$ for N defect modes in a periodic medium.

Figure 2A shows the complex band structures for the ΓX direction and real band structures for an SC with a point defect. In our case, we use only one direction of incidence to analyze the complex band structure because the localized mode appears at the same frequency for all the incidence directions. The supercell used for the calculations is shown in the inset of Figure 2A.

Analyzing the real band structures (propagating properties) we can observe that the localized mode appears at 920 Hz (green dashed line). For frequencies in the BG, the borders of the point defect act as perfect mirrors and produce the localized mode in this cavity. Figure 2B presents the numerical results of the acoustic field inside a point defect in a SC in complete good agreement with the experimental data. Figure 2C represents the measurements of the localized mode in a cavity obtained for the first time.

In Figure 2A, the complex bands give information about the evanescent behaviour of the localized mode. We observe that a complex band obtained by EPWE becomes a purely real for the localized mode (green dashed line). The value exactly coincides with the one obtained by PWE with supercell approximation. The border of the cavity is located at approximately $x=0.6$ m as it can be observed in Figure 2B. Figure 2D presents both numerical (blue line) and experimental (blue open squares) values of the acoustic field from the end of the cavity to the end of a SC, showing the evanescent behaviour of the localized mode outside the cavity.

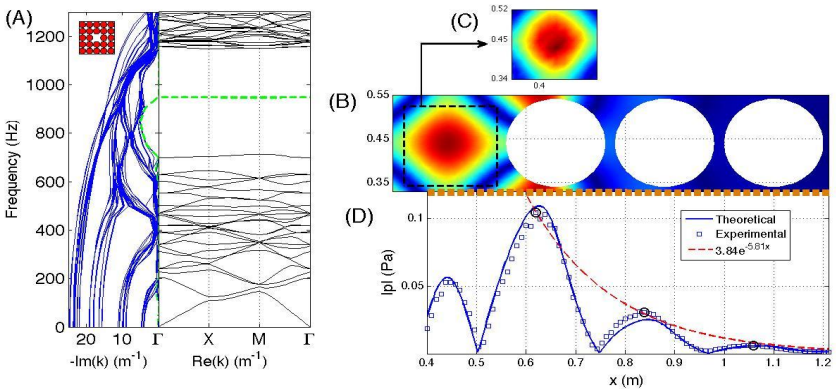

Figure 2 Evanescent behaviour of a localized mode in a point defect. (A) Complex (Blue lines) and Real (black lines) bands structures for a SC made of rigid scatterers with a point defect. Square periodicity $a=0.22$ m and radius $r=0.1$ m. (B) Numerical prediction of the acoustic field inside the point defect at the localization frequency, 920 Hz. (C) Experimental measurement of the localized field inside the point defect. (D) Analysis of the evanescent behaviour of the localized mode. Blue continuous line (Open blue squares) represents the numerical predictions (experimental data) of the acoustic field in the path between two rows of cylinders containing the point defect marked with a broad orange dashed line. Red dashed line shows the fitting of the exponential like decay of the localized mode.

The propagation of waves inside periodic structures consists on both propagating and evanescent modes. This work could well become fundamental for the correct understanding of the design of narrow filters and waveguides based on periodic media with point defects.

References

[1] Y.C. Hsue, A.J. Freeman and B.Y. Gu. *Phys. Rev. B*, **72**, 195118, (2005).
[2] V. Laude, Y. Achaoui, S. Benchabane and A. Khelif. *Phys. Rev. B*, **80**, 092301, (2009).
[3] J.D. Joannopoulos, R. D. Meade, and J.N. Winn, *Molding the Flow of Light*, Princeton University Press, USA (1995).

Phononics 2011: First International Conference on Phononic Crystals, Metamaterials and Optomechanics
Santa Fe, New Mexico, USA, May 29-June 2, 2011
PHONONICS-2011-0102

Interaction between Periodic Arrays and Finite Impedance Surface: Analytical Results and Experimental Data

V. Romero-García[1,2], J.V. Sánchez-Pérez[2]; K. Attenborough[3], S. Taherzadeh[3]; A. Chong[3], A. Krynkin[4]; O. Umnova[4];

[1] *Instituto de Ciencia de Materiales de Madrid, Consejo Superior de Investigaciones Científicas, Spain*
virogar1@gmail.com
[2] *Centro de Tecnologías Físicas: Acústica, Materiales y Astrofísica. Universidad Politécnica de Valencia, Cno de Vera s/n 46020 Valencia, Spain*
virogar1@upvnet.upv.es, jusanc@fis.upv.es
[3] *Department of Design, Development, Environment and Materials. The Open University Walton Hall Milton Keynes MK7 6AA United Kingdom*
k.attenborough@open.ac.uk, s.taherzadeh@open.ac.uk, y.b.a.chong@open.ac.uk
[4] *School of Computing, Science & Engineering The University of Salford, Salford,Great Manchester, M5 4WT. United Kingdom*
a.krynkin@salford.ac.uk, O.Umnova@salford.ac.uk

Abstract: The design of devices based on phononic crystals seems a hot topic nowadays. However, there are some effects that have to be into account for the development of their technology, as for instance the existence of a close surface that could interfere with their acoustic properties. We present here an analytical model to analyze this interaction based on the Multiple Scattering Theory in good agreement with experimental data.

The acoustic interaction between both the scattered field produced by a phononic crystal (PC) and the reflected field from a line source in a finite impedance surface is reported in this work. This interference pattern is analyzed using an analytical model, based on the multiple scattering theory[1,2], called by us Image Multiple Scattering Theory (IMST). The analytical predictions have been compared with experimental data showing good agreement. We have considered throughout this work a line source and the case of cylindrical scatterers in air. Although the most interesting situation is likely to involve periodic arrays of cylinders with their axes perpendicular to the surface, this would require solution of a 3D problem. Therefore we have considered the tractable 2D problem involving a periodic array of cylinders with their axes parallel to the surface.

This analytical method developed in this work modifies the classical Multiple Scattering Theory using the method of images in order to add the reflected field on the finite impedance surface. According to this methodology, two sources have been considered: the real source located in the real space and an image source located in the image space. Moreover, the image of the real array is also considered to solve the problem. In Figure 1 (left panel), we represent the real case for a square array of cylinders with lattice constant *a,* and radius *r*. In Figure 1 (right panel) we show the scheme of images: one can observe the real space XY with the real array of scatterers and the real source O, and the image space (XY´) with the image array of scatterers and the image source O´.

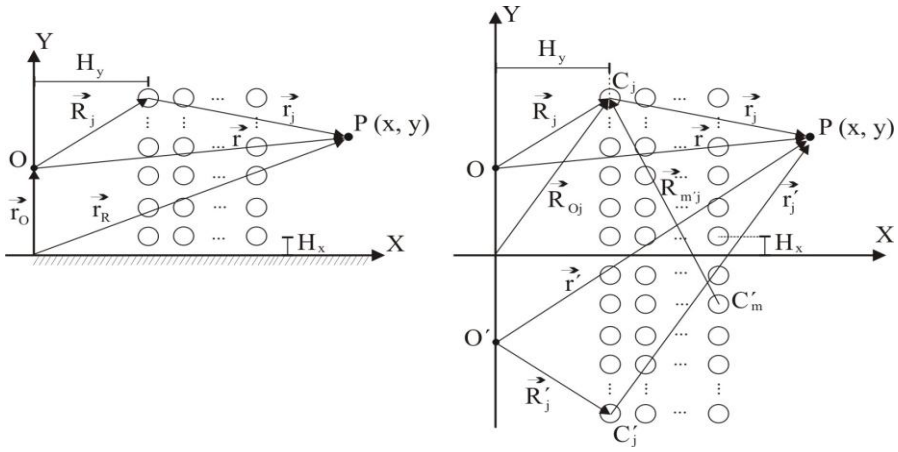

Figure 1 Left panel: Array of scatterers in the real case. Right panel: scheme of the method of images for the array of the left panel.

To add the effect of the surface in our analytical scattering model, we have characterized

Phononics 2011: First International Conference on Phononic Crystals, Metamaterials and Optomechanics
Santa Fe, New Mexico, USA, May 29-June 2, 2011
PHONONICS-2011-0102

it by means of the reflection coefficient $R(r_O,r_C;\ v)$ of the surface. If $R(r_O,r_C;\ v)=1$ we are in the case of acoustically hard ground but, generally speaking, $R(r_O,r_C;\ v)$ will be a function that will depend on the positions of both the source and the receiver and on the frequency. Specifically $R(r_O,r_C;\ v)$ can be characterized by the finite impedance of the surface. In this work, the finite impedance surface is represented by a two parameter impedance model[3]:

$$Z_{ground} = \rho c_0 (0.434 \sqrt{\frac{\sigma_e}{f}} (1+i) + 9.75 i \frac{\sigma_e}{f}) \tag{1}$$

Taking into account these considerations, the total acoustic field obtained using the IMST is:

$$P(\vec{r}) = H_0(kr) + R(\vec{r}_O, \vec{r}_C; f) H_0(kr') + \sum_{m=1}^{M} \sum_{l=-L}^{L} A_l^m (H_l^{(1)}(kr_m) e^{il\theta_m} + R(\vec{r}_O, \vec{r}_C; f) H_l^{(1)}(kr_{m'}) e^{-il\theta_{m'}}) \tag{2}$$

Where M is the total number of the scatterers in the real space. The analytical Insertion Loss (IL) spectra for an array of cylinders placed over a soft plane are studied. The characteristics of the considered system are: *21* rigid cylinders with $r=0.055$ m arranged in a square array with $a=0.069$ m and with the bottom row placed near to a finite impedance surface with σ_e = *4000* Pa s/m^2 and α_ε = *105* m^3. The line source is placed at point O = *(0, 0.235)* m. The distance between the source and the array is $d=0.755$ m. In Figure 2 we can observe the comparison between measured and calculated the IL in three points, with coordinates at (A) *(1.203, 0.117)* m, (B) *(1.203, 0.235)* m and (C) *(1.203, 0.352)* m. The agreement between analytical predictions and experimental data are fairly good.

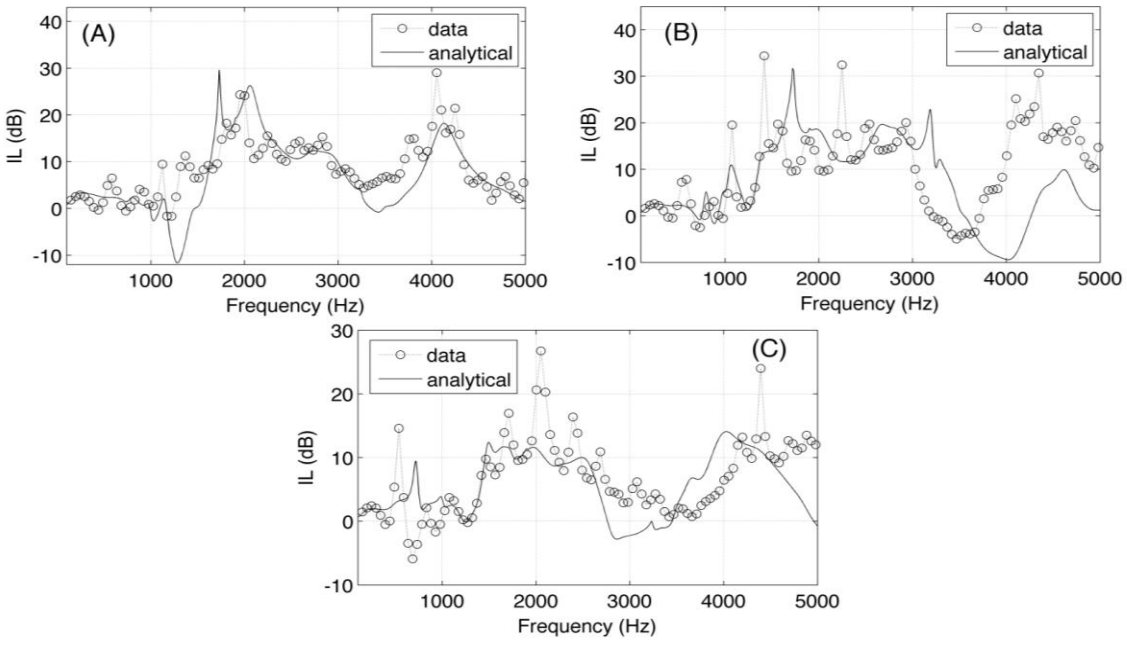

Figure 2 Measured and predicted Insertion Loss spectra for the three points indicated in the text.

This model can be applied in several technological applications of PC as for instance in the case of the design of acoustic barriers based on arrays of scatterers, where the effect of the excess attenuation produced by the reflected wave by the ground has a great influence on the acoustical properties of the PC.

References

[1] P.A. Martin, *Multiple Scattering: Interaction of Time-Harmonic Waves with N Obstacles*, Cambridge University Press, UK (2006).
[2] Y. Y. Chen and Z. Ye, *Phys. Rev. E* **64**, 036616 (2001).
[3] S. Taherzadeh and K. Attenborough, *J. Acous. Soc. Am.* **105**, 2039 (1999).

Phononics 2011: First International Conference on Phononic Crystals, Metamaterials and Optomechanics
Santa Fe, New Mexico, USA, May 29-June 2, 2011
PHONONICS-2011-0107

Lattice Materials: A Unified Structural Mechanics Perspective

A. Srikantha Phani

Department of Mechanical Engineering, 6250 Applied Science Lane, The University of British Columbia, Vancouver, BC, V6T 1PZ, CANADA,
srikanth@mech.ubc.ca

Abstract: Lattice materials with a periodic microstructure are suitable for multifunctional structures with high specific stiffness, favourable acoustic and thermal properties. Their mechanical response under static and dynamic loads is considered from a unified structural mechanics perspective combining Bloch wave theory with Finite Element Method.

Lattice materials possess a spatially repetitive unit cell geometry on the length scales of a few millimetres [1–5]. Typical applications include sandwich beams, panels and space trusses [6]. It has been observed that the unit cell geometry has a profound influence upon their macroscopic mechanical response [2] under static and dynamic loading conditions [7]. Optimal design of lattice microstructures for wave bearing properties such as bandgaps have been studied [8]. Ideas from solid state physics [9] have been combined with structural mechanics principles [10,11] and applied to periodic *structural* systems for aerospace applications. This interdisciplinary approach has lead to significant insights, most notably the exposition of Anderson localisation phenomena in macro scale periodic structures [12]. More recent studies [7,13,14] approach lattice and phononic materials in the spirit of earlier pioneering works in periodic structure theory [10,11].

Response/Phenomenon	Loading Type	Deformation Type	Remarks
Passband [7]	Dynamic	Spatially extended	Linear, infinite, perfect lattice material
Stopband (Bandgap) [7]	Dynamic	Spatially localised	Linear, infinite, perfect lattice material
Saint Venant effects [15]	Static	Spatially localised	Linear, finite, perfect lattice material with a boundary or interface
Rayleigh waves [15]	Dynamic	Spatially localised	Linear, finite, perfect lattice material with a boundary or interface
Anderson Localisation [12]	Dynamic	Spatially localised	Linear, imperfect lattice material
Discrete Breathers [16,17]	Dynamic	Spatially localised	Nonlinear, perfect lattice material in the weak coupling limit

Table **1** A classification of mechanical response of lattice materials. Here a perfect lattice material contains no defects such as cracks, whereas an imperfect lattice material does. Symmetries present in the perfect lattice are perturbed or destroyed in the imperfect lattice.

A unified structural mechanics perspective on mechanical response of lattice materials viewed as a periodic network of beams will be presented. Two distinct regimes of mechanical response are identified: in spatially extended response regime the entire lattice can sustain deformation; deformation can be confined to a spatially localised region due to defects, interfaces, and nonlinearity. A wide range of phenomena can be incorporated within this perspective as shown in Table 1.
Eigenvalue problems using Bloch theory will serve to unify the spatially localised and spatially extended deformation phenomena in Table 1 for linear systems. A quadratic eigenvalue problem proposed in an earlier work [15] to study elastic boundary layers will be revisited and generalised to include surface waves of Rayleigh type. Numerical results will be provided for one-dimensional linear nonlinear systems. Interaction between the defects and nonlinearity will be highlghted.

Phononics 2011: First International Conference on Phononic Crystals, Metamaterials and Optomechanics
Santa Fe, New Mexico, USA, May 29-June 2, 2011
PHONONICS-2011-0107

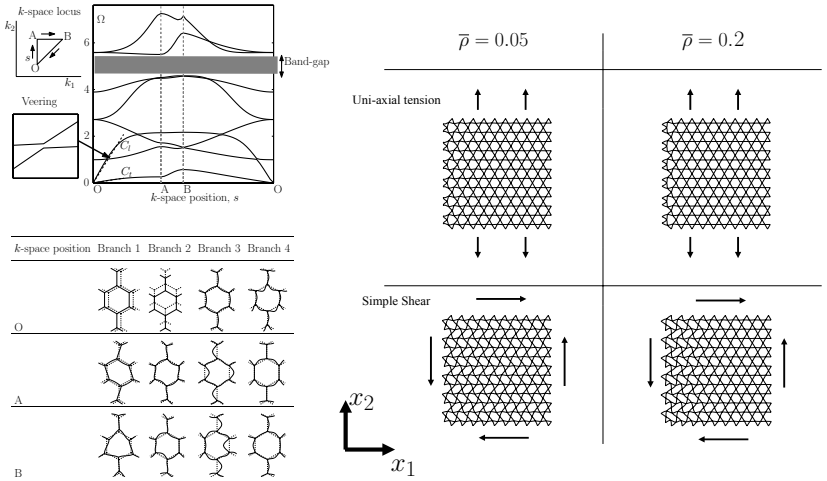

Figure **1** Dispersion curves for a hexagonal lattice exhibiting bandgaps and curve veering (left)[7]; Elastic boundary layers of Saint Venant type in a Kagome lattice subjected to stretching and shear deformations (right)[15]: $\overline{\rho}$ denotes relative density.

Acknowledgement: Financial support from Natural Sciences and Engineering Research Council (NSERC) of Canada through the award of Discovery Grant and support from Canada Research Chairs (CRC) program and Canada Foundation for Innovation (CFI) are thankfully acknowledged.

References

1 M.F. Ashby and L.J. Gibson, *Cellular solids: structure and properties*, Cambridge University Press, UK, (1997).

2 N.A. Fleck, V.S. Deshpande, and M.F. Ashby, Micro-architectured materials: past, present and future, *Proceedings of the Royal Society of London, Series A*, **466**, 2495–2516, (2010).

3 W.E. Warren and A.M. Kraynik, Foam mechanics: the linear elastic response of two-dimensional spatially periodic cellular materials, *Mechanics of Materials*, **6**, 27–37, (1987).

4 R.M. Christensen, Mechanics of cellular and other low density materials, *International Journal of Solids and Structures*, **37**(1), 93–104, (2000).

5 R.S. Lakes, Foam structures with a negative Poisson's ratio, *Science*, **235**, 1038–1040, (1987).

6 N. Wicks, and J.W. Hutchinson, Optimal truss plates, *International Journal of Solids and Structures*, **38**, 5165–5183, (2001).

7 A.S. Phani, J. Woodhouse, N.A. Fleck, Wave propagation in two-dimensional periodic lattices, *Journal of the Acoustical Society of America*, **119**(4), 1995–2005, (2006).

8 O. Sigmund and J.S., Jensen, Systematic design of photonic band-gap materials and structures by topology optimization, *Proceedings of the Royal Society of London, Series A*, **361**, 1001–1019, (2003).

9 C. Kittel, *Elementary solid state physics: a short course*, John Wiley & Sons, inc., USA, (1962).

10 D.J. Mead, Wave propagation in continuous periodic structures: research contributions from Southampton 1964-1995, *Journal of Sound and Vibration*, **190**(3), 495–524, (1996).

11 R.S. Langley, N.S. Bardell, and H.M. Ruivo, The response of two-dimensional periodic structures to harmonic point loading: a theoretical and experimental study of a beam grillage, *Journal of Sound and Vibration*, **207**(4), 521–535, (1997).

12 C.H. Hodges, and J. Woodhouse, Vibration isolation from irregularity in a nearly periodic structure: theory and measurements, *Journal of the Acoustical Society of America*, **74**, 894–905, (1983).

13 M. Ruzzene, F. Scarpa, F. Soranna, Wave beaming effects in two-dimensional cellular structures, *Smart Materials and Structures*, **12**, 363–372, (2003).

14 M. I. Hussein, Reduced Bloch mode expansion for periodic media band structure calculations, *Proceedings of the Royal Society of London, Series A*, **465**, 2825–2848, (2009).

15 A.S. Phani, and, N.A. Fleck, Elastic Boundary Layers in Isotropic Periodic Lattices, *ASME: Journal of Applied Mechanics*, **75**(2), 021020–021027, (2008).

16 R.S. Mackay, and, S. Aubry, Proof of existence of breathers for time-reversible or Hamiltonian networks of weakly coupled oscillators, *Nonlinearity*, **7**, 1623–1643, (1994).

17 S. Aubry, Discrete Breathers: Localization and transfer of energy in discrete Hamiltonian nonlinear systems, *Physica D*, **216**, 1–30, (2006).

Phononics 2011: First International Conference on Phononic Crystals, Metamaterials and Optomechanics
Santa Fe, New Mexico, USA, May 29-June 2, 2011
PHONONICS-2011-0117

Phononic Crystals with Applications to Sound and Vibration Control

Jihong Wen

Key Laboratory of Photonic and Phononic Crystals of Ministry of Education, and Institute of Mechatronical Engineering, National University of Defense Technology, Changsha, Hunan 410073, P.R. China
wenjihong@vip.sina.com

Abstract: A two dimensional binary locally resonant phononic crystal (PCs) has been fabricated and thoroughly analyzed. A lumped-mass method has been proposed as an efficient tool to calculate the band structure of PCs. The concept of PCs is introduced into the design of beam and plate structures, and the acoustic materials to improve their vibration and sound performance.

The propagation of acoustic/elastic waves in periodic composite materials known as phononic crystals (PCs) has received considerable attention in recent years. The emphasis is placed on the existence of band gaps within which acoustic/elastic waves are all forbidden. Moreover, when point defects or linear/planar defects are introduced into perfect PCs, acoustic/elastic waves within band gaps will be restricted to the point defects or can only propagate along the linear/planar defects. Such unique properties of PCs are of great interest in the field of confinement, waveguiding and filtering, as well as the area of noise and vibration isolation.

Since the year 2001, funded by the State Key Development Program for Basic Research of China and the National Science Foundation of China, we started research work on PCs and their applications in the area of sound and vibration control. Our research interests focused on the band gap formation mechanisms, band gap calculation methods and potential applications in vibration and noise reduction.

1. Band gap formation mechanism

A crucial foundational problem involved in the investigations of PCs is to gain a clear understanding of the band gap formation mechanisms. Two kinds of mechanisms have been developed: Bragg reflection mechanism and locally resonant (LR) mechanism. Resonance gaps formed by the LR mechanism can be tuned to a very low frequency range with a far smaller lattice constant than that governed by the Bragg condition.

A thorough study has been carried out on the Bragg reflection mechanism and we have revealed the resonance modes near the edges of the first absolute band gap in a two-dimensional (2D) PC with a matrix of epoxy, which lead to a wide band gap. The resonance of the upper band edge is induced by Bragg scattering, and the resonance is mainly concentrated in the matrix. The lower edge resonance is induced by the joint effects of the Bragg and Mie scattering and presents a rotary resonance mode. The gap induced by the rigid-body resonance coalesces with the Bragg gap, so a wider gap comes into being.

The previous LR PCs are all ternary systems, which consist of a cubic array of coated spheres immersed in epoxy or of a lattice of coated cylinders in epoxy (the coatings are thin films of soft rubber). In contrast, we fabricate a 2D binary LR PC composed of periodic soft rubber cylinders immersed in epoxy host. A comprehensive study has been performed. Numerical simulations predict that subfrequency gaps also appear because of the high contrast of mass density and elastic constant of the soft rubber. The LR mechanism in forming the subfrequency gaps is thoroughly analyzed.

Generally, the Bragg reflection mechanism and the locally resonant mechanism focus on the effects of the periodic structure and the single unit cell respectively. We have developed a model including these two factors simultaneously. Through analysing the elastic wave modes in 2D PCs by MST, the uncoupling effects between the differently ordered cylindrical wave components have been identified at the edge of the band gaps. For the uncoupled modes of the lowest gap, a simple analytic expression is presented, which comprises the Mie scattering of a single unit cell and the effects of the periodic structure simultaneously. A comprehensive physical insight into the formation mechanism of the band

Phononics 2011: First International Conference on Phononic Crystals, Metamaterials and Optomechanics
Santa Fe, New Mexico, USA, May 29-June 2, 2011
PHONONICS-2011-0117

gaps is provided, no matter the band is derived of Bragg reflection or local resonance. In addition, a clear physical understanding of the formation of full band gaps is also proposed.

2. Band gap calculation methods

Several theoretical methods have already been developed for the calculation of band structures of PCs. Mostly, the calculations are based on the plane-wave expansion (PWE) method, in which the wave equations are solved in Fourier space. Nevertheless, PCs involving media with a large contrast in their elastic/density properties are not easy to treat with PWE because a large number of plane waves are required to obtain reliable band structures. Other methods such as the variational method and the finite difference time domain algorithms overcome the convergence problem in a certain extent. The multiple scattering theory (MST) has advantages in convergence. However, it can only handle specific arrays of spheres (3D) or cylinders (2D) up to now and complicated mathematical deductions are always required.

A lumped-mass method that works in the direct space based on the discretization of continuous systems has been proposed by us as a new way to compute the band structure of PCs. We conclude that the lumped-mass method converges faster and its convergence is insensitive to the sharp variation of elastic constants on the interfaces inside the PCs. Especially, the latter advantage is unique in comparison with other studies on the improvement of plane-wave expansion methods. Another unique feature of the new method is that it needs not deduce the structure factors for every inerratic shape thus it can be used to deal with PCs with any unit shapes directly.

3. Applications in vibration and noise reduction

The investigations on PC materials/structures are driven partly by their potential applications such as wave filters, vibrationless environments for high-precision systems, transducer design, etc. By introducing the idea of PCs into the design of engineering structures, such as beams and plates, band gaps can be achieved to control the transmission of vibrations. Vibration band gaps in these structures, based on either the Bragg reflection mechanism or the locally resonant mechanism, have been found theoretically and experimentally. Furthermore, the characteristics of directional propagation of elastic waves in 2D PCs within specific pass band frequencies has be studied and utilized to control the direction of the vibration transmission. These studies provide new ideas for the application of PCs in the field of structural vibration control.

The idea of localized resonance in PCs is introduced to improve the low-frequency acoustic absorption of viscoelasitc materials. Both the theoretical results and the experimental measurements show the phenomenon of low-frequency absorption. The outputs of our work may be useful for tailoring the acoustic absorption properties and are expected to have applications in underwater acoustic absorption materials.

Phononics 2011: First International Conference on Phononic Crystals, Metamaterials and Optomechanics
Santa Fe, New Mexico, USA, May 29-June 2, 2011
PHONONICS-2011-0121

Using classical FEM to predict the dynamical response of periodic devices in acoustic and vibration applications

Miguel M. Neves[1], Olavo M. J. Silva[2], Hugo Policarpo[3], António G. Cartaxo[3]

[1] IDMEC-IST, DEM, TULisbon, Av. Rovisco Pais, 1049-001Lisboa, Portugal., maneves@dem.ist.utl.pt,
[2] Laboratory of Acoustics and Vibration, Federal University of Santa Catarina, Brazil olavo@lva.ufsc.br,
[3] DEM, TULisbon, Av. Rovisco Pais, 1049-001Lisboa, Portugal., hugo.policarpo@ist.utl.pt, antonio.cartaxo@sapo.pt

Abstract: The task of predicting the dynamical response and tailoring wave propagation filters for practical frequency ranges is here presented. Finite element steady-state analysis is performed on periodic devices of finite length considering periodic distribution of materials, addition of masses to a tube and periodic curvatures. Validation obtained with prototypes, one for attenuation of axial vibration and other for sound propagation, is also mentioned.

Four periodic devices were studied for passive control of elastic wave propagation. Analytical, numerical and experimental results were obtained to verify and validate the models used. In the first example, it is considered the case of the dynamical characterization of the axial harmonic response (U) at one end of a multi-laminated periodic bar. The bar is excited by an axial harmonic force (F) at the other end (see Fig. 1). Design of such devices can be found in literature, see for e.g. in Hussein et al.[1]. In order to have the device working within a frequency range of interest, it was recommended to use a periodic sequence of cells built from steel and cork agglomerate. The main purpose of this material choice was to play with the high contrast in the wave propagation speeds. This is done to maximize vibration attenuation regions present where predictable stop-bands regions are known to exist for the case of infinite periodic structures. Experimental results confirmed the predicted attenuation regions (for details see, Policarpo et al.[1]).

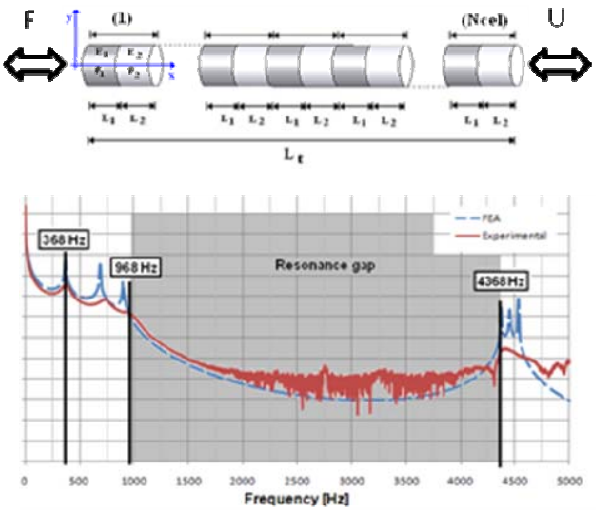

Figure 1 At the top, distribution of two material components along the rod. At the bottom, predicted (FEA) and experimental responses.

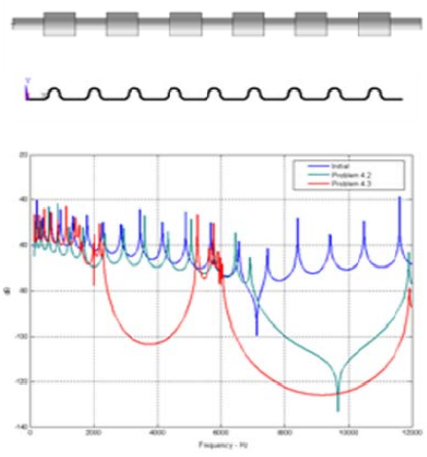

Figure 2 At the top, straight hollow tubes with periodically repeated diameter or curvature. At the bottom: harmonic responses from the periodic tubes and from a straight hollow tube of constant diameter (for the same weight, length and internal diameter).

The second and third examples are from a similar attenuation problem for the flexural vibrations at one end of a hollow shaft excited by a transversal force at the other end. A straight tube with periodically repeated piecewise constant diameter (also seen as added masses) is presented in the second problem. For the third case, the tube is defined as a sequence of periodically-repeated

Phononics 2011: First International Conference on Phononic Crystals, Metamaterials and Optomechanics
Santa Fe, New Mexico, USA, May 29-June 2, 2011
PHONONICS-2011-0121

curvatures (see Fig. 2). Although authors found this parametrization interesting for some pratical applications, it was not found in scientific literature. The corresponding frequency response graphics illustrate practical improvements of their response in comparison to the equivalent straight hollow tube of the same length, weight and internal diameter. For the sake of simplicity, the FE models were limited to the elastic bar (i.e., link or rod elements) and to Euler-Bernoulli beams, but in principle the algorithms used can be applied to shells and solids as well.

As a last example, sound transmission through a periodically spaced array of steel cylinders (Fig. 3) was also studied for comparison between analytical, numerical and experimental results (obtained in an anechoic chamber). It required the building of two classical FE models and a prototype. First, a Fluid-Structure Interaction (FSI) modeled by a finite element technique is used to analyze the case of a wave propagating in the air through a periodic distribution of cylinders perpendicular to the direction of the wave propagation. Second, the FSI is deactivated, resulting in a model with only an acoustic fluid with fixed holes instead of the cylinders. The experiments confirmed that the prototype exhibits strong sound attenuation bands at the frequencies predicted in literature (Sánchez-Pérez et al. [2]). The effect is considerably well reproduced by means of numerical simulations (in this case, for the frequency range of 1250 up to 1750 kHz). Experimental results with the prototype in an anechoic chamber confirmed the predicted attenuation.

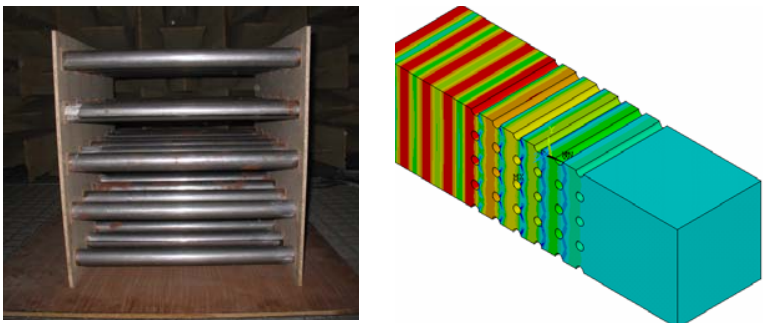

Figure 3 Left: A photo of the experimental device built from a periodically spaced array of metallic cylinder elements in air. Right: A plot of the air pressure distribution predicted from the harmonic FE analysis considering a plane wave at the entry and anechoic boundary condition at the exit.

In conclusion, the use of classical finite elements with harmonic (steady-state) analysis allowed to correctly predict the behavior of these simple devices. Although frequencies were not very low, the frequency ranges were considered of interest for engineering applications. The results showed a good correlation with the predictions of the corresponding Bloch wave analysis, as long as the number of finite elements used per wavelength is adequate. Simple finite element meshes were used. Experimental tests performed at axial vibration devices and at the set of parallel cylinders shown good correlation with the numerical predictions. It is expected that these contributions can make it easier for engineers to understand and to use the advantages of the actual phononics knowledge.

Acknowledgements
This study received financial support from FCT (Portuguese Science Foundation) through the project PTDC/EME-PME/71488/2006 (NM) and IDMEC-IST (Portugal).

References
[1] M. I. Hussein, G. M. Hulbert, and R. A. Scott, Dispersive elastodynamics of 1D banded materials and structures: design. *J Sound Vib* **307**:865-893 (2007).
[2] H. Policarpo, M.M. Neves, A.M.R. Ribeiro, Dynamical response of a multi-laminated periodic bar: Analytical, numerical and experimental study, *SHOCK AND VIBRATION*, **17** (4-5), 521-535 (2010).
[3] J. V. Sánchez-Pérez, D. Caballero, R. Mártinez-Sala; C. Rubio; J. Sánchez-Dehesa; F. Meseguer; J. Llinares; F. Gálvez; Sound Attenuation by a Two-Dimensional Array of Rigid Cylinders, *Physical Review Letters*, **80** (24), 5325-5328 (1998).

Phononics 2011: First International Conference on Phononic Crystals, Metamaterials and Optomechanics
Santa Fe, New Mexico, USA, May 29-June 2, 2011
PHONONICS-2011-0123

Dynamical effective properties of elastic multilayers

O. Poncelet[1], A. N. Norris[1,2], A. L. Shuvalov[1], A. A. Kutsenko[1]

[1] Université de Bordeaux, CNRS UMR 5295, I2M, Talence, France
olivier.poncelet@u-bordeaux1.fr, alexander.shuvalov@u-bordeaux1.fr, kucenkoa@rambler.ru
[2] Mechanical & Aerospace Engineering, Rutgers University, Piscataway NJ, USA
norris@rutgers.edu

Abstract: Based on the state-vector formalism, a material with the Willis type of constitutive relations is recovered as the model of an homogeneous dispersive effective medium that emulates periodic multilayered or graded materials. The effective material constants are defined through the actual physical parameters in the form, which is not, in principle, restricted to low frequency and which can reveal both the dispersion and the stopbands. Some examples for the out-of-plane case are provided.

The state-vector formalism and the wave number matrix K

The state-vector formalism is well-suited for describing elastic waves in anisotropic 1D-heterogeneous media with density $\rho(y)$ and stiffness tensor $c_{ijkl}(y)$. Consider quasi-plane modes with the phase factor $\exp \mathrm{i}(k_x x - \omega t)$, where ω is the frequency and k_x the wavenumber in an arbitrarily chosen direction X orthogonal to Y. Taking the Fourier transforms of the equilibrium ($\sigma_{ij,i} = \rho \ddot{u}_j$) and stress–strain ($\sigma_{ij} = c_{ijkl} e_{kl}$) equations in all variables except y leads to an ordinary differential system for the state vector $\boldsymbol{\eta}(y) = \left(\mathbf{u}(y) \quad \mathrm{i}\mathbf{n}\boldsymbol{\sigma}(y)\right)^{\mathrm{T}}$:

$$\frac{\mathrm{d}}{\mathrm{d}y}\boldsymbol{\eta}(y) = \mathbf{Q}(y)\boldsymbol{\eta}(y), \quad \mathbf{Q}(y) = \mathrm{i}\begin{pmatrix} k_x \mathbf{N}_1 & \mathbf{N}_2 \\ k_x^2 \mathbf{N}_3 - \rho\omega^2 \mathbf{I} & k_x \mathbf{N}_1^{\mathrm{T}} \end{pmatrix}, \quad \begin{array}{l} \mathbf{N}_1 = \mathbf{N}_4^{\mathrm{T}} = -(nn)^{-1}(nm) \\ \mathbf{N}_2 = -(nn)^{-1} \\ \mathbf{N}_3 = (mm) - (mn)(nn)^{-1}(nm) \end{array} \tag{1}$$

where $\mathbf{m}$ and $\mathbf{n}$ denote the unit vectors parallel to X and Y, and $(nn)_{jk} = n_i c_{ijkl} n_l$, $(nm)_{jk} = n_i c_{ijkl} m_l = (mn)_{kj}$, $(mm)_{jk} = m_i c_{ijkl} m_l$. Given the initial condition at some $y_0 (\equiv 0)$, the solution to system (1) is $\boldsymbol{\eta}(y) = \mathbf{M}(y,0)\boldsymbol{\eta}(0)$, where $\mathbf{M}(y,0)$ is the 6×6 matricant evaluated by the product of the matrix exponentials of the homogeneous layers or more generally by the Peano series in case of a graded material[1].

Now let ρ, c_{ijkl} and hence $\mathbf{Q}$ depend on y periodically with a period T. In this case the central role is played by the matricant $\mathbf{M}(T,0)$ over the unit cell $[0,T]$ which is called the monodromy matrix. For instance, $\mathbf{M}(T,0) = \prod_n^{j=1} \mathrm{e}^{\mathbf{Q}_j d_j}$ for a piecewise homogeneous (layered) medium. The wavenumber matrix $\mathbf{K}$ is introduced by denoting $\mathbf{M}(T,0) = \exp(\mathrm{i}\mathbf{K}T)$ whence $\mathrm{i}\mathbf{K} = \frac{1}{T}\ln \mathbf{M}(T,0)$. For relatively low frequency, it can be evaluated as $\mathrm{i}\mathbf{K} = \langle \mathbf{Q} \rangle + \Sigma_{m=1}^{\infty} \mathrm{i}\mathbf{K}^{(m)}$ where $\langle\cdot\rangle$ denotes the average over a period and $\mathbf{K}^{(m)}$ are the matrix coefficients of the Magnus expansion of matrix logarithm ($\mathbf{K}$ is thereby defined in the first Brillouin zone that corresponds to the zeroth Riemann sheet of $\ln z$ with a cut $\arg z = \pm\pi$).

Dynamic homogenization and constitutive equations

Formally, $\exp(\mathrm{i}\mathbf{K}y)$ is a solution to equation (1) with the actual matrix of coefficients $\mathbf{Q}(y)$ replaced by the constant matrix $\mathrm{i}\mathbf{K}$. This motivates the concept of an effective homogeneous medium, whose material model admits the wave equation in the form (1) with a constant system matrix $\mathbf{Q}_{eff} \equiv \mathrm{i}\mathbf{K}$. Dynamic properties are realized by taking $\mathbf{Q}_{eff} = \mathrm{i}\mathbf{K}$ beyond the zero-order term $\langle \mathbf{Q} \rangle$ that describes the quasi-static limit only. It turns out[2] that the dispersive density matrix $\boldsymbol{\rho}^{(eff)}$ and elastic tensor $c_{ijkl}^{(eff)}$ of the effective medium must be complemented by a stress-impulse coupling that leads to the motion and constitutive equations in the Willis form:

$$\sigma_{ij,i} = \dot{p}_j, \qquad \sigma_{ij} = c_{ijkl}^{(eff)} e_{kl} + S_{ijr}\dot{u}_r, \qquad p_q = S_{klq} e_{kl} + \rho_{qr}^{(eff)} \dot{u}_r, \tag{2}$$

where $\mathbf{p}$ is the vector of momentum density, and $S_{ijk} = S_{jik}$ is the Willis coupling tensor[4]. The effective material constants $c_{ijkl}^{(eff)}(\omega)$, $S_{ijr}(\omega)$ and $\rho_{qr}^{(eff)}(\omega)$ can be expressed via the actual material properties $c_{ijkl}(y)$ and $\rho(y)$.

Phononics 2011: First International Conference on Phononic Crystals, Metamaterials and Optomechanics
Santa Fe, New Mexico, USA, May 29-June 2, 2011
PHONONICS-2011-0123

Examples for the case of SH waves in a periodically bilayered medium

We illustrate the general formulation by considering SH waves propagating in a periodic structure of isotropic unit cells. In this case, the out-of-plane effective constitutive relations are as follows:

$$\sigma_{13} = c_{55}^{(eff)} u_{,1} + c_{54}^{(eff)} u_{,2}\,, \qquad \sigma_{23} = c_{45}^{(eff)} u_{,1} + c_{44}^{(eff)} u_{,2} + S_{43}\dot{u}\,, \qquad p_3 = S_{43} u_{,2} + \rho^{(eff)}\dot{u}\,. \tag{3}$$

If the unit cell consists of two homogeneous isotropic layers, then the effective material parameters involved in (3) can be found beyond the low-frequency range in an exact form of transcendental functions of unrestricted ω and k_x, see Ref. 2. Figure 1 shows these effective parameters computed for the normal propagation ($k_x = 0$) through the periodic stack of layers $j = 1,2$ of equal thickness ($d_j = \frac{1}{2}$) with $\rho_1 = 1$, $c_1 = 1$ and $\rho_2 = 2$, $c_2 = 2$, where $c_i = \sqrt{\mu_i / \rho_i}$ is the shear wave speed. The vanishing of both $c_{44}^{(eff)}$ and $\rho^{(eff)}$ at the band edge at $\omega = \omega_1 \approx 2.6$ is expected on the basis of the fact that $\mathbf{Q}_{eff}$ is singular at the band edge and scales as $(\omega - \omega_1)^{-1/2}$ near it[3]. The square root decay of both $c_{44}^{(eff)}$ and $\rho^{(eff)}$ is apparent in figure 1.

As an example of the type of boundary problem that can be solved using the effective medium equations, consider reflection–transmission of SH waves at a bonded interface $y = 0$ between the half-space of the periodically stratified medium ($y > 0$) and a uniform half-space ($y < 0$) of isotropic material with ρ_0 and $c_0 = \sqrt{\mu_0 / \rho_0}$. An SH wave is incident from the uniform half-space with propagation direction at angle θ from the interface normal. The total solution is taken as $u(x,y) = e^{\mathrm{i}k_x x}\left(e^{\mathrm{i}k_y y} + Re^{-\mathrm{i}k_y y}\right)$ for $y \le 0$ and $u(x,y) = Te^{\mathrm{i}k_x x}e^{\mathrm{i}K(\omega,k_x)y}$ for $y \ge 0$, with $(k_x, k_y) = \omega / c_0\,(\sin\theta, \cos\theta)$. Taking into account the continuity conditions for displacement and traction at $y = 0$ yields the reflection and transmission coefficients R and T in the standard form $R = (Z_- - Z_+)/(Z_- + Z_+)$ and $T = 2Z_-/(Z_- + Z_+)$, where $Z_- = \rho_0 c_0 \cos\theta$ is the impedance in the uniform half-space and $Z_+ = \omega^{-1}\left(Kc_{44}^{(eff)} + k_x c_{45}^{(eff)} - \omega S_{43}\right)$ is the impedance for the effective medium equivalent to the periodic half-space. It is noteworthy that the effective impedance Z_+ is identical to the impedance of the actual periodic material because they both imply a ratio of components of the outgoing eigenvector that is common for $\mathbf{M}(T,0)$ and $\mathbf{K}$. Thus the above solution for the reflection and transmission coefficients, which is expressed via the effective material parameters, is an exact result. Figure 2 shows its calculation for the case of normal incidence.

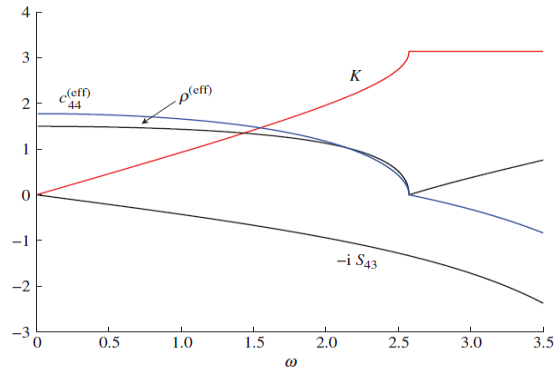

Figure 1 The effective material constants of Eq. (2) at $k_x = 0$ (elastic in blue, inertial in black) for the periodically bilayered medium (see its parameters in the text). The vertical wavenumber is added (in red). The frequency range includes the first band edge which is at the frequency where $\mathrm{Re}\,K = \pi$ first occurs. Only the real parts of the quantities indicated are plotted (for ω in the stopband the imaginary parts of $c_{44}^{(eff)}$, $\rho^{(eff)}$ and K are non-zero but not shown).

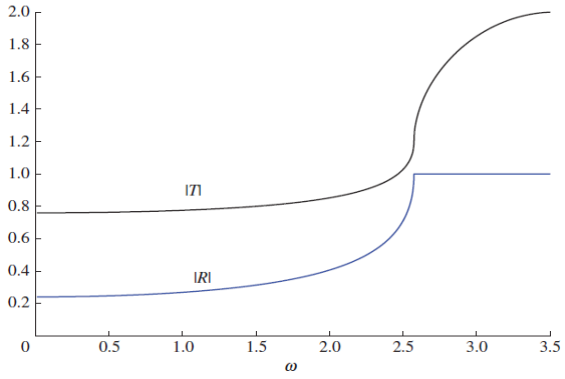

Figure 2 The magnitude of the reflection and transmission coefficients $|R(\omega)|$ and $|T(\omega)|$ for normal incidence ($\theta = 0$ or $k_x = 0$) from a uniform half-space with $\rho_0 = 1$, $c_0 = 1$ on a periodically bilayered structure which was used in figure 1. As expected, $|R| \le 1$ with total reflection in the stopband.

References

[1] M. C. Pease-III, *Methods of matrix algebra*, Academic Press, New-York, NY (1965).
[2] A. L. Shuvalov, A. A. Kutsenko, A. N. Norris, and O. Poncelet, *Proc. R. Soc. A,* doi:10.1098/rspa.2010.0389 (2011).
[3] A. L. Shuvalov, A. A. Kutsenko, and A. N. Norris, *Wave Motion* **47**, 370–382 (2010).
[4] G. W. Milton, and J. R. Willis, *Proc. R. Soc. A* 463, 855–880 (2007).

Phononics 2011: First International Conference on Phononic Crystals, Metamaterials and Optomechanics

Santa Fe, New Mexico, USA, May 29-June 2, 2011

PHONONICS-2011-0137

Structurally-Inspired Phononic Metamaterials

Gregory M. Hulbert[1] , Julien Meaud[1], Zheng-Dong Ma[1]

[1] Department of Mechanical Engineering, University of Michigan, Ann Arbor, MI 48109-2125, USA, hulbert@umich.edu, jmeaud@umich.edu, mazd@umich.edu

Abstract: The distinction between materials and structures has blurred. The development of phononic metamaterials based upon novel structural systems is considered in this work. In particular, a Negative-Poisson Ratio (NPR) structure is used as the foundation for developing phononic metamaterials comprising a 'structural' framework of stiff material and a more compliant material that can dissipate energy.

The distinction between materials and structures, has, in the past decade, become blurry. In a recent publication[1] that received some publicity, the discovery of ice crystals on the moons of Saturn and Neptune exhibit negative linear compressibility, also known as Negative-Poisson Ratio (NPR) response and negative thermal expansion. The underlying molecular structure shown resembles mechanism-like topologies. In the context of phononics, dispersive behavior exhibited by materials[2-4] motivated the development of structurally-based systems with the ability to mitigate energy propagation through structures[5-7].

Inspired by the progess in phononic metamaterials and the applications of NPR materials[8], we recently began investigating the development of phononic metamaterials based upon novel structural systems. In particular, a Negative-Poisson Ratio (NPR) structure is used as the foundation for developing phononic metamaterials comprising a 'structural' framework of stiff material and a more compliant material that can dissipate energy. The goal of this work is to model, analyze and design NPR structures at different length scales with an aim towards creating structurally-based materials, which can be manufactured practically at the sub-millimeter scale.

Figures 1 and 2 depict two baseline structural topologies that exhibit significantly different effective Poisson ratios. The configuration of Figure 1 has an effective Poisson ratio of -0.8 while that of Figure 2 is -7.5. The loading direction is considered as vertical with the effective response measured laterally. Figure 3 shows one of the baseline topologies, including the void space filled with a soft, polymer fill.

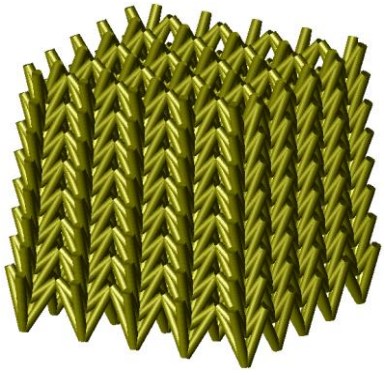

Figure 1 NPR structural configuration with $\nu = -0.8$

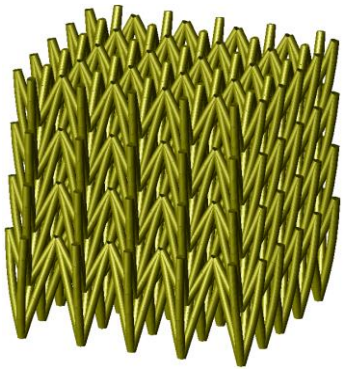

Figure 2 NPR structural configuration with $\nu = -7.5$

Phononics 2011: First International Conference on Phononic Crystals, Metamaterials and Optomechanics
Santa Fe, New Mexico, USA, May 29-June 2, 2011
PHONONICS-2011-0137

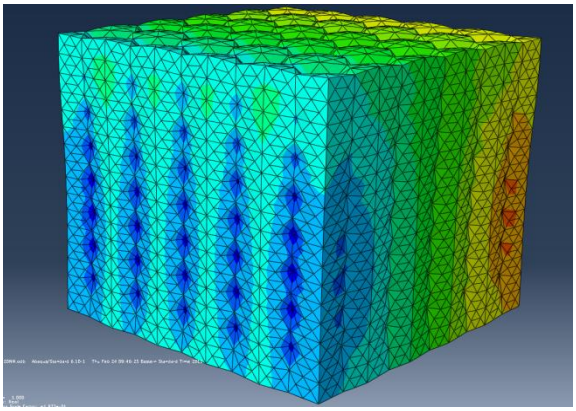

Figure 3 NPR structural configuration with polymer fill

The dynamic response of the NPR-based material/structural concepts is computed using a unit cell analysis for both the void and polymer filled architectures. The effective performance of these concepts is assessed for energy attenuation across frequency bases, with consideration of different cell sizes associated with a structural-sized unit cell and with a unit cell size on the millimeter or smaller scale.

References

[1] A.D. Fortes, E. Suard, and K.S. Knight, *Science*, **331**, 742-746 (2011).
[2] M.I. Hussein, G.M. Hulbert, and R.S. Scott, *JSV,* **289**, 779-806 (2006).
[3] M.I. Hussein, G.M. Hulbert, and R.S. Scott, *JSV,* **307**, 865-893 (2007).
[4] M.I. Hussein, K. Hamza, G.M. Hulbert, and K. Saitou, *Waves in Random and Complex Media,* **17**, 491-510 (2007).
[5] E. Dede, and G.M. Hulbert, *IJNME,* **73**, 470-492 (2008).
[6] E. Dede, and G.M. Hulbert, *JSV,* **313**, 493-509 (2008).
[7] E. Dede, and G.M. Hulbert, *FEAD,* **44**, 819-830 (2008).
[8] Y. Liu, and Z.-D. Ma, IMECE 2007, **10B**, 965-973 (2008).

Phononics 2011: First International Conference on Phononic Crystals, Metamaterials and Optomechanics
Santa Fe, New Mexico, USA, May 29-June 2, 2011
PHONONICS-2011-0148

Longitudinal Vibration Band Gaps in Rods with Periodically Attached Multi-Degree-of-Freedom Vibration Absorbers

Yong Xiao, Jihong Wen, Xisen Wen

Institute of Mechatronical Engineering, and Key Laboratory of Photonic and Phononic Crystals of Ministry of Education, National University of Defense Technology, Changsha 410073, China
xiaoyong.nudt@gmail.com

Abstract: Band gap behavior in rods with periodically mounted multi-degree-of-freedom resonators (vibration absorbers) is concerned. Explicit expressions are derived for the calculation of complex band structures. The effects of absorber parameters on the band gap properties are studied. The band gap formation mechanisms of the system are explained by analytical models with explicit formulations.

Band gap characteristics of uniform rods with periodically attached multi-degree-of-freedom (MDOF) resonators (or call "vibration absorbers" in the context of mechanical engineering) are investigated. The system considered is sketched in Figure 1.

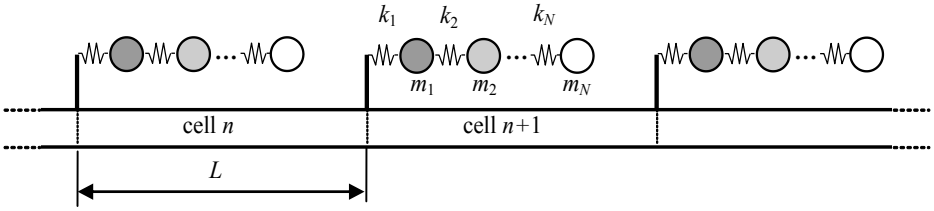

Figure 1 An infinite uniform rod with periodically attached MDOF vibration absorbers.

Using the well-known transfer matrix method, explicit formulation is derived for the calculation of complex band structures of the system

$$\cosh(\pm\mu) = \cos(\beta L) + (\bar{D}/2)\sin(\beta L) \tag{1}$$

where μ is the so-called propagation constant [1, 2], β is the wavenumber for the longitudinal waves in the rods, $\bar{D}$ is the non-dimensional dynamic stiffness of the absorber. Generally, the band gap behaviour can be well represented by the attenuation constant, $\mathrm{Re}(\mu)$, which can be mathematically described by a multivariable function as

$$\mathrm{Re}(\mu) = f(E, A, \rho, L, \omega, m_0, k_1, m_1, k_2, m_2, ...) = \mathrm{Re}\left\{\mathrm{acosh}[\cos(\beta L) + (\bar{D}/2)\sin(\beta L)]\right\} \tag{2}$$

It is demonstrated that both Bragg-type and resonance-type band gaps co-exist in the system. Multiple desired resonance gaps can be achieved due to the multiple natural frequencies of the MDOF absorbers. This is different from the case of single-degree-of-freedom (SDOF) absorber attachments, which produces only one tunable resonance band gap.

The effects of absorber parameters on the band gap behaviour are studied by employing the so-called "attenuation constant surface (ACF)", as first introduced in Ref.[3]. For example, the parametric influence analysis for locally resonant rods with 2DOF absorbers can be performed by employing the following bivariable function

Phononics 2011: First International Conference on Phononic Crystals, Metamaterials and Optomechanics
Santa Fe, New Mexico, USA, May 29-June 2, 2011
PHONONICS-2011-0148

$$\mathrm{Re}(\mu) = f(\omega, k_1)\big|_{k_1 \in (k_{1,\min}, k_{1,\max})} \tag{3}$$

For convenience, the spring stiffness can be nondimensionalized as $\mathrm{K}_1 = k_1/(EA/L)$, and a nondimensional frequency can be defined as $\Omega = \beta L/\pi$. Two numerical examples of ACF defined by Equation (3) are shown in Figure 2. In the first example, the resonance frequencies of the absorber, i.e. Ω_1 and Ω_2, are both tuned to well below the first Bragg condition, thus two low frequency resonance gaps around these frequencies can be achieved. In the second example, the first absorber frequency is set below the first Bragg condition, while the second one it tuned to be equal to the Bragg condition (i.e., $\Omega_2 = 1$). It can be

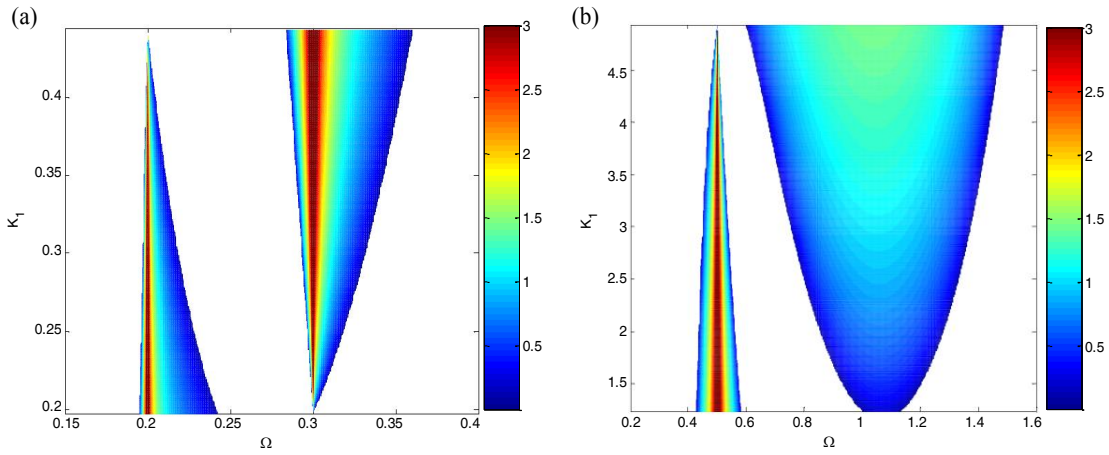

Figure 2 Attenuation constant surfaces of locally resonant rods with 2DOF absorb**ers**. **(a)** $\Omega_1 = 0.2$, $\Omega_2 = 0.4$; **(b)** $\Omega_1 = 0.5$, $\Omega_2 = 1$. The mass ratio of the absorbers is fixed to be $\gamma = 0.5$.

seen band gap coupling phenomenon occurs in this case, giving rise to a super-wide coupled band gap. Such a unique property can be utilized in the broadband control of wave propagation in rods. According to the ACS plots depicted in Figure 2, the width of the band gaps can be adjusted by varying the designing parameter k_1.

Finally, in order to explain the band gap behaviour of the system, both rigorous derivations and physical models are provided to understand the band gap formation mechanisms. Exact expressions are obtained to predict all the band edge frequencies as well as the band gap coupling conditions directly, without the calculation of band gaps.

References

[1] D.J. Mead, *J. Sound Vib*, **27**. 236-260 (1973).
[2] D.J. Mead, *J. Sound Vib*, **319**. 282-304 (2009).
[3] Y. Xiao, B.R. Mace, J. Wen, and X. Wen, *Phys. Lett. A*, **375**, 1485-1491 (2011).

Phononics 2011: First International Conference on Phononic Crystals, Metamaterials and Optomechanics

Santa Fe, New Mexico, USA, May 29-June 2, 2011

PHONONICS-2011-0166

Intensity-Dependent Dispersion in Nonlinear Phononic and Photonic Layered Systems

Kevin L. Manktelow[1] , Michael Leamy[1], Massimo Ruzzene[1]

[1] George W. Woodruff School of Mechanical Engineering, Georgia Institute of Technology, 771 Ferst Drive N.W. Atlanta, GA 30332, USA,

kevin.manktelow@gatech.edu, michael.leamy@me.gatech.edu, massimo.ruzzene@ aerospace.gatech.edu

Abstract: Intensity-dependent dispersion relationships of nonlinear phononic and photonic layered systems are produced. Analysis techniques common in optics are applied to phononic systems, and a recently introduced perturbation approach for discrete phononic systems is applied to optical systems after a finite element discretization. The results are validated with numerical simulation and show that both approaches may be beneficial for system analysis.

Structures with periodically varying geometry and material properties are known to exhibit advantageous wave propagation properties such as negative refractive indices, frequency band gaps and spatial beaming. Periodic layering of materials with differing mass and stiffness properties produces phononic crystals, which tailor elastic and acoustic wave propagation. The optical analogue of phononic crystals is the photonic crystal which is typically formed by periodic layering of materials with alternating permittivity.

Phononic and photonic crystals are typically considered to operate in regimes where a linear constitutive relationship (e.g., stress-strain) provides an adequate representation. For high intensity wave propagation, however, weak nonlinearities can affect performance. For example, a cubic nonlinearity gives rise to frequency shifting and thus a shift in band gap location. In the study of nonlinear optics, a cubic term has been treated using a quasi-linear constitutive relationship with intensity dependent properties. This nonlinearity is known as the Kerr nonlinearity and gives rise to a refractive index proportional to intensity. This technique is explored herein for generating nonlinear dispersion relationships for the elastic case. In addition, a perturbation method developed previously for discrete elastic systems, used in conjunction with a finite element discretization, is proposed as an alternative dispersion analysis tool in both photonic and phononic systems.

One of the simplest phononic or photonic crystals is a one-dimensional bilayered material, consisting of alternating material layers with contrasting properties. This type of structure exhibits many of the interesting properties of more complex photonic or phononic crystals such as non-trivial dispersion and band gaps. Phononic and photonic systems with linear constitutive relationships are governed by the same one-dimensional wave equation. The nonlinear constitutive laws typically employed for phononic and photonic systems result in different nonlinear terms in the fully nonlinear wave equations.

When nonlinearities are excluded from the analysis, an analytical dispersion relation may be obtained succinctly using the transfer matrix method. The transfer matrix method is also applicable to the nonlinear bilayered rod when quasi-linear intensity-dependent material properties replace the full nonlinear model. In this work, the bilayered material system is first discretized using a Galerkin weighted-residuals approach. The discretized system is then analyzed with (1) a linear stress-strain relationship, (2) a quasi-linear stress-strain relationship and the transfer matrix approach, and (3) a perturbation analysis of the fully nonlinear governing equations. The perturbation approach results in fundamentally different band gap structure in some cases and predicts a frequency shift which is less than that estimated by the quasi-linear transfer matrix approach.

Phononics 2011: First International Conference on Phononic Crystals, Metamaterials and Optomechanics

Santa Fe, New Mexico, USA, May 29-June 2, 2011

PHONONICS-2011-0166

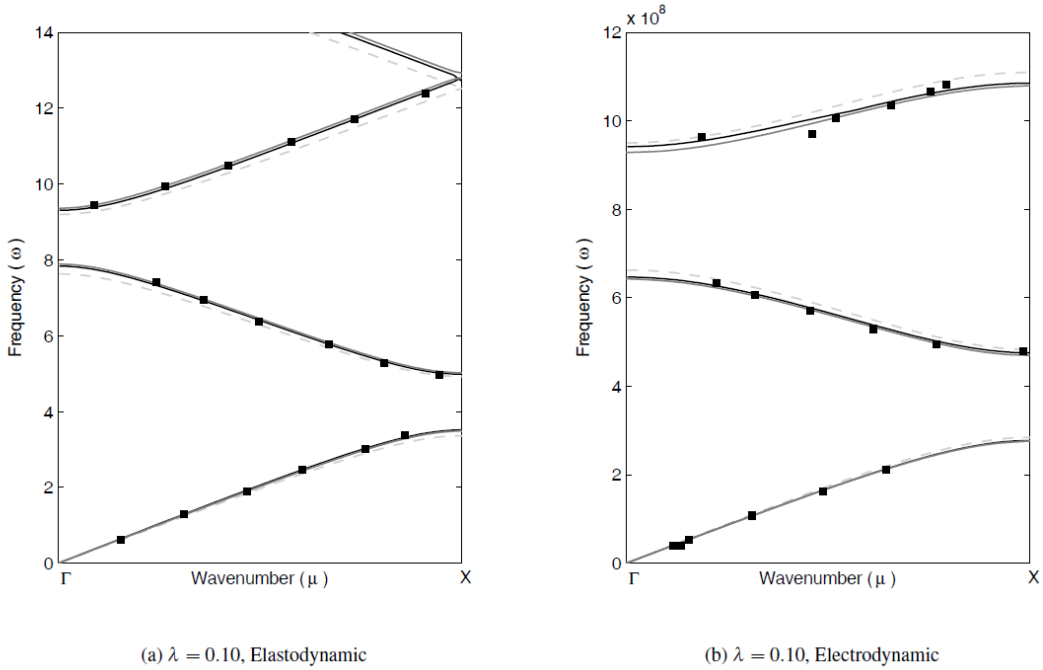

Figure 1. Dispersion band structure for (a) Phononic layered material, and (b) Photonic layered material at relatively large nonlinearities. Dispersion curves are drawn for systems with linear material properties (light-gray dashed), quasi-linear material properties applied using the transfer matrix method (solid dark gray), and fully nonlinear material properties analyzed using finite element discretization and perturbation analysis (solid black). Black markers indicate the results of transient finite element simulations.

Numerical simulations using the fully nonlinear finite element equations are included for validation of the predicted dispersion curves. Numerical simulations are performed using the discretized model over a domain large enough to be considered infinite. The resulting space-time data is analyzed using a two-dimensional discrete Fourier transform to obtain wavenumber/frequency data points. The results show good agreement with the perturbation approach, and indicate that it may provide a simple and accurate framework for the design and optimization of nonlinear phononic and photonic band gaps.

Phononics 2011: First International Conference on Phononic Crystals, Metamaterials and Optomechanics
Santa Fe, New Mexico, USA, May 29-June 2, 2011
PHONONICS-2011-0177

Characterization of Band Gap Resonances in Finite Periodic Structures

Andrew S. Tomchek, Edgar A. Flores, Liao Liu, Bruce L. Davis, Mahmoud I. Hussein

Department of Aerospace Engineering Sciences, University of Colorado at Boulder, CO 80309, USA
andrew.tomchek@colorado.edu, edgar.flores@colorado.edu, liao.liu@colorado.edu, bruce.davis@colorado.edu, mih@colorado.edu

Abstract: While resonant propagation modes are non-existent within band gaps in infinite periodic structures, it is possible for anomalous band-gap resonances to appear in finite periodic structures as a result of the periodicity truncation. We establish two criteria for the characterization of band-gap resonances and propose an approach for their elimination. By considering flexural periodic beams, we show that as the number of unit-cells is increased the vibration response corresponding to band-gap resonances (1) does not shift in frequency, and (2) drops in amplitude. Both these outcomes are not exhibited by regular pass-band resonances, nor by resonances in finite homogenous beams when the length is changed. Our conclusions stem from predictions based on Timoshenko beam theory coupled with matching experimental observations.

We consider a periodic beam structure composed of alternating layers of Aluminum (Al) and the polymer ABS. First we utilize Bloch theory, and following a Bloch FE formulation[1,2] we compute the band structure of an infinite periodic structure. This calculation shows that three relatively large band gaps exist between 0 and 9 kHz, as shown in Fig. 1 (top). In order to study the finite-size effects, we seek an FRF for the same periodic structure with a finite number of unit-cells. Fig. 1 (bottom) shows this result obtained theoretically (solid line) and experimentally (dashed line) for a 5-unit-cell beam in which the "input" force excitation and the "output" displacement evaluation are at the extreme ends of the structure. We observe that a clear anomalous resonance peak exists well inside the second band gap. We refer to this as a band-gap resonance. To distinguish between this type of resonance and regular pass-band resonances, we increase the number of unit-cells in the finite structure and note the effects on all the resonances within our covered frequency range of 0-9 KHz. The results are shown in Fig. 2, from both theory and experiment. First we observe in Fig, 2 (top) that the frequency of the band-gap resonance does not shift as the number of unit-cells is incremented from 5 to 6, while in contrast the frequencies of all the regular pass-band resonances experience clear shifts. Second we observe in Fig. 2 (bottom) that the amplitude of the band gap resonance drops significantly as the number of unit-cells in increased from 5 to 15, while the amplitudes of all the regular pass-band resonances do not experience any noticeable drops. These two traits can be used as criteria for the characterization of band-gap resonances.

We next examine the sensitivity of the frequency values corresponding to band-gap resonances to smooth variations in the unit-cell geometric configuration. In the baseline configuration considered above, the length-fraction of ABS in the unit-cell is $a_{ABS}/a = 0.2$, where a_{ABS} denotes the length of the ABS polymer layer. This length-fraction is now varied over that full range $0 \le a_{ABS}/a \le 1$, which at one extreme ($a_{ABS}/a = 0$) represents a homogenous Al beam, and at the other extreme ($a_{ABS}/a = 1$) represents a beam composed of only ABS polymer. Fig. 3 shows the resonances (solid thin lines) of a 5 unit-cell structure as a function of a_{ABS}/a. Experimental results corresponding to an ABS length-fraction of 0.1, 0.15, 0.2, 0.25 and 0.3 are shown as discrete data points (dots). Superimposed in the figure, are the boundaries of all band gaps (solid thick lines) as determined from the application of Bloch theory to corresponding infinite periodic structures. The band-gap resonances, characterized by the two criteria mentioned above, appear inside the band-gap boundaries. It can be seen that the band-gap resonances are noticeably more sensitive to varying the unit-cell layer dimensions than the regular pass-band resonances. Once they exit the band gaps however, these unique resonances become less sensitive to varying a_{ABS}/a, and their sensitivity becomes similar to that of the regular resonances. Furthermore, once outside the band gaps these resonances no longer appear to satisfy the first criterion outlined above, thus losing their uniqueness and transforming to regular pass-band resonances them-

Phononics 2011: First International Conference on Phononic Crystals, Metamaterials and Optomechanics
Santa Fe, New Mexico, USA, May 29-June 2, 2011
PHONONICS-2011-0177

selves. To investigate the effect of unit-cell length (and hence total length of a finite periodic structure) on band-gap resonances, we varied a while keeping $a_{ABS}/a = 0.2$. The results, which are shown in the inset of Fig. 3, indicate that the relative location of a band-gap resonance within a band gap is independent of the unit-cell (or full structure) size. We conclude that varying the topology of the unit cell can be used as an approach for eliminating band gap resonances that arise due to periodicity truncation.

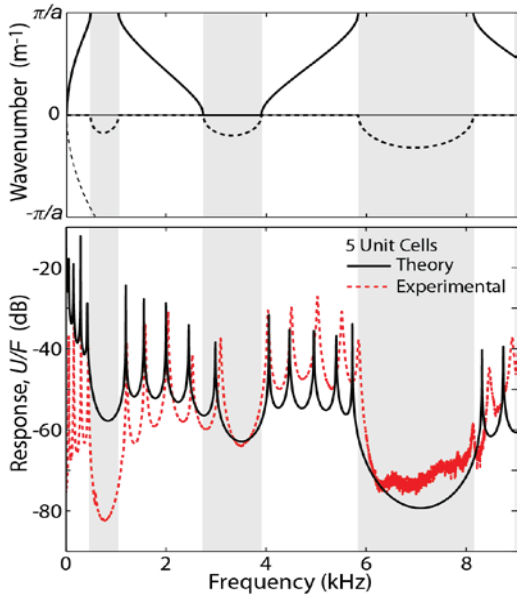

Figure 1. Frequency band diagram of the infinite version of the periodic beam structure (top), and FRF results for the finite periodic beam structure (bottom). In the top sub-figure, the solid line represents propagation modes, and the dashed line represents attenuation modes. The band gaps corresponding to the frequency band structure are shaded in grey in both sub-figures.

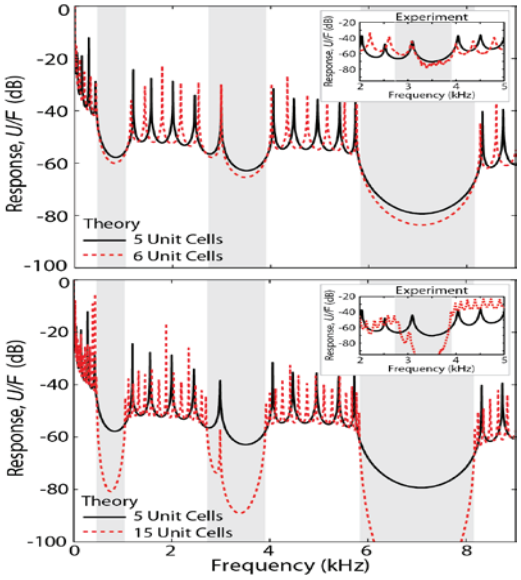

Figure 2. FRF comparison for finite periodic beam structure with different number of unit-cells. The results show that band-gap resonances do not shift in frequency (top) and drop in amplitude (bottom) as the number of unit cells is increased.

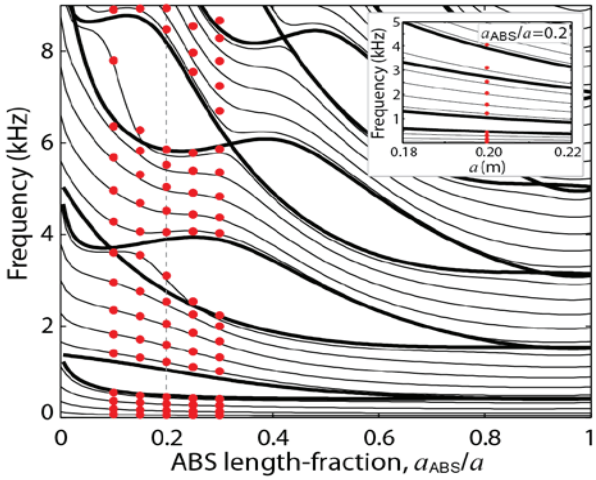

Figure 3. Resonance frequency (thin solid lines, theory; dots, experiment) versus ABS length-fraction for 5-unit-cell finite periodic beam structures. Inset: Resonance frequency (thin solid lines, theory; dots, experiment) versus unit-cell length, a, for a 5-unit-cell periodic beam structure. The thick solid lines in both the main figure and the inset represent the boundaries of the band gaps for corresponding infinite periodic structures.

References

[1] Hussein, M. I., *Proc. R. Soc. A*, **465**, pp. 2825-2848 (2009).
[2] L. Liu and M. I. Hussein, *Seventeenth International Conference on Sound and Vibration,* pp. 1- 7 (2010).